Quantum Control of a Single Qubit

Agata Maria Brańczyk

A thesis submitted for the degree of
Bachelor of Science with Honours in Physics
The University of Queensland

June, 2005

Declaration

This thesis is an account of research undertaken between July 2004 and June 2005 at the Department of Physics, the University of Queensland, Brisbane, Australia, under the supervision of Dr. Alexei Gilchrist and Dr. Stephen Bartlett.

Except where acknowledged in the customary manner, the material presented in this thesis is, to the best of my knowledge, original and has not been submitted in whole or part for a degree at any university.

Agata M. Brańczyk

June, 2005

Acknowledgements

I would like to thank my awesome supervisors: Alexei Gilchrist and Steve Bartlett, for taking me on for this project and for all their time, support and guidance throughout the year. I would also like to thank everyone who contributed to this project and the writing of this thesis, especially: Andrew Doherty for helpful discussions; Jeremy O'Brien, Geoff Pryde and Andrew White for their experimental expertise; and Nicole Gilchrist, Paulo Mendonca and Timo Nieminen for proof reading numerous drafts of this thesis. I would like to thank Mark Dowling, who didn't directly contribute to this project, but whose help and advice over the last few years can not go without mention. Thanks to the honours students in room 301 for making this year a lot more fun, if not a little more insane. Thanks to my family, for being great over the past year and not minding too much that I've been neglecting them, especially toward the end. And last, but by no means least, a special thank-you to Simon Parkin for his patience, support, advice and understanding.

Abstract

We present and analyse a theoretical proposal to demonstrate quantum control of a single qubit. Quantum control is the measurement and correction of a quantum system. The quantum system is measured, and the dynamics of the system are altered, based on the measurement results. In classical control, it is of benefit to acquire as much information about the system as possible. This is not the case with quantum control, as any measurement of the system results in back-action noise due to the measurement. *In quantum control it is possible to know too much.* We perform a theoretical characterisation of the performance of the quantum control scheme in protecting the quantum state from noise and investigate the optimal measurement strength. Our scheme is compared with two alternative approaches: doing nothing to measure or correct the system; or using a classical-like discriminate-and-replace scheme. The optimality of the quantum control scheme is also investigated. Finally, we propose a prototype experiment to demonstrate this scheme with polarisation encoded photonic qubits.

Contents

List of Figures

Chapter 1

Introduction

Feedback control is integral to the development of most modern technologies. It is responsible for the stable operation of complex devices that would otherwise be unstable due to disturbances, noise, variability in fabrication of parts, and many other imperfections.

As devices get smaller, they enter a regime where their behaviour becomes quantum mechanical in nature. Rather than search for ways to avoid these quantum behaviours, we can try to use them to our advantage to make further technological advances. For example, quantum computers rely on such quantum behaviours and would benefit from smaller features in solid state systems. Quantum systems are known to be even more susceptible to noise than classical systems and they will require some form of control. We will see in this thesis that classical control will not suffice and that a new theory, a theory of *quantum* control, will need to be developed.

In this thesis, an experimentally feasible scheme to demonstrate the quantum control of a single qubit is proposed. Before this can be done, we must cover a number of necessary concepts. A basic introduction to classical control and the theory of quantum measurements is given in this chapter. The concepts from these two sections are then used when we introduce quantum control. The chapter finishes with a review of previous work conducted in theoretical and experimental quantum control.

1.1 Classical Control

Control is the measurement and alteration of a system based on the results of the measurement. Much of today's technology relies on the stabilisation of inherently unstable systems. This is done by making a measurement on that system, then feeding back the information gained from the measurement, to alter the system based on the measurement results. This process can be carried out repeatedly or continuously.

An example of a device which uses control is the thermostat. When on an oven is turned on and set to a certain temperature T, a signal is sent to a device in the oven which runs a current through the element. When the temperature reaches T, the thermostat sends a signal to switch off the current. After some time the temperature begins to fall and the thermostat sends another signal to switch on the current which runs through the element, which increases the temperature in the oven again. This process is repeated while the oven remains turned on. The thermostat can in principle measure the temperature with arbitrary accuracy. In fact, the more accurate the measurement, the better the control scheme.

This example demonstrates the main ideas behind classical control: measurement, feedback and correction. In classical physics, we want to gain as much information about a system as possible. When formulating the theory of quantum control we will need to take some ideas from classical control. However, the important difference in quantum physics is that the measurement of a system will disturb its state. Therefore, in quantum control we need to find a way to make measurements on a system without disturbing it too much. In pursuing this goal we will make use of *weak measurements*: measurements which allow us to gain adequate information about a system without disturbing it more than is necessary.

Before moving onto quantum control, we first need to introduce some properties of quantum measurements.

1.2 Quantum Measurement

In this section, we will discuss a number of quantum measurements including the weak measurements that will be used in the quantum control scheme. The concept of distinguishability in quantum mechanics is also introduced.

1.2.1 Projective Measurements

A projective measurement is a measurement which projects a system onto an eigenspace of an *observable* M. The observable has the following spectral decomposition:

$$M = \sum_m P_m \tag{1.1}$$

where P_m is the projector onto the eigenspace of M with eigenvalue m [1].

If we were to measure the state $|\psi\rangle$, the probability of getting the result m would be given by

$$p_m = \langle\psi|P_m|\psi\rangle \tag{1.2}$$

and given that the outcome m occurred, the state of the system immediately after measurement is

$$\frac{P_m|\psi\rangle}{\sqrt{p_m}}\,. \tag{1.3}$$

We will sometimes use the phrase, 'to measure in a basis $\{|m\rangle\}$'. This means to perform a projective measurement with projectors $P_m = |m\rangle\langle m|$, as opposed to some other decomposition of M.

For rank-one projectors, the post-measurement state is $|m\rangle$. Consider an example of a projective measurement on the single qubit state $|\phi\rangle = (|0\rangle + |1\rangle)/\sqrt{2}$. If we were to make a measurement on the state in the computational basis (measure in the basis $\{|0\rangle, |1\rangle\}$) then the probability of getting the outcome 0 is

$$\begin{aligned} p_0 &= \langle\phi|P_0|\phi\rangle && (1.4)\\ &= \left(\frac{\langle 0| + \langle 1|}{\sqrt{2}}\right)|0\rangle\langle 0|\left(\frac{|0\rangle + |1\rangle}{\sqrt{2}}\right) && (1.5)\\ &= \frac{1}{2}\,. && (1.6) \end{aligned}$$

Similarly $p_1 = 1/2$. Given that the measurement result was 0, the state of the system immediately after measurement is

$$\begin{aligned} \frac{P_0|\phi\rangle}{\sqrt{p_0}} &= \frac{|0\rangle\langle 0|\frac{|0\rangle+|1\rangle}{\sqrt{2}}}{\sqrt{\frac{1}{2}}} && (1.7)\\ &= |0\rangle\,. && (1.8) \end{aligned}$$

Similarly, if the measurement result was 1, the state of the system immediately after measurement is $|1\rangle$.

1.2.2 QND Measurements

In quantum mechanics, any measurement that acquires information about a system must necessarily disturb that system. Quantum non-demolition (QND) measurements allow for this type of measurement to be made by keeping the back action noise entirely within unwanted observables [2].

The standard way to perform a QND measurement is to employ the use of a *meter* system. By coupling the system to be measured (the *signal* system) to the meter system, the states become entangled. By performing a measurement of the meter system, we can acquire information about the signal system due to the entanglement

between the two systems [2].[1]

Typically, QND measurements are projective, which means that even though the measurements do not destroy the state of interest, they still alter the state by collapsing it into an eigenstate of the observable [3].

1.2.3 Weak Measurements

It was shown by Pryde *et al.* [4] that by employing the use of a controlled-NOT (CNOT) gate, which we will define in the next section, it is possible to perform a QND measurement, on a single qubit, with variable strength. We are calling this type of measurement a *weak measurement*.

A weak measurement can be made by varying the level of entanglement between the signal and meter states. When the states are completely entangled and the meter state is measured, a projective measurement with maximum measurement strength (a QND measurement) is made on the signal state. If the entanglement is varied such that the signal and meter states are no longer entangled, then the measurement of the meter state provides no information about the signal state and does not disturb the state of the system. This is essentially a weak measurement with the measurement strength 'turned off'. By varying the measurement strength, there is a trade-off between the amount of information one can gain about a system and the disturbance to that system.

In the quantum control scheme proposed in this thesis, the state of the meter is rotated *after* the entanglement. This does not vary the level of entanglement between the states — it varies the measurement basis of the meter, essentially enabling us to 'ignore' the entanglement between the states when we make the measurement.

1.2.4 Distinguishability

If one attempts to distinguish between two non-orthogonal states, there is no way that this can be done with certainty due to the laws of quantum physics. Consider two non-orthogonal states of a qubit:

$$|0\rangle \quad \text{and} \quad |+\rangle \equiv \frac{|0\rangle + |1\rangle}{\sqrt{2}}\,. \tag{1.9}$$

These two states can not be distinguished with certainty because the state $|+\rangle$ can be decomposed into a non-zero component parallel to $|0\rangle$ and an orthogonal component

[1] Note that in the implementation example, when we use quantum optics, the meter and signal states will be photons. This means that the measurement on the meter photon will have to be a destructive measurement because all optical measurements are based on photodetection.

to $|0\rangle$ [1]. If we measure in the $\{|0\rangle, |1\rangle\}$ basis, then a measurement of $|0\rangle$ will always give the result 0; and a measurement of $|+\rangle$ will give the result 0 with probability 1/2 and the result 1 with probability 1/2. If we make our measurement and the result is 1, then we can determine that the state was $|+\rangle$ (it could not have been $|0\rangle$); however if the result is 0, then we have no way of knowing which state we measured. If we try to make the measurement in the $\{|+\rangle, |-\rangle\}$ basis, then the same problem arises as the measurement of $|0\rangle$ will give the result '+' with probability 1/2 and the result '−' with probability 1/2.

In quantum control, we want to measure a system and correct the state of the system, based on the measurement results. If the system can be in one of two non-orthogonal states, then this measurement will not distinguish between these two states with certainty.

1.3 Quantum Control

In classical physics, there is no fundamental reason why a control scheme would not want to acquire as much information about a system as possible. This is not the case in quantum physics. The very act of measuring the system will necessarily disturb it due to *back-action* noise resulting from the measurement [5, 6]. We saw from the example in section 1.2.1 that a measurement on the state $|\phi\rangle$ could give the result 1 or 0 with equal probability. The measurement result gives only some information about the state before the measurement. Any information we acquire about the system will not completely describe the original state of the system since it will be different from the state it was in before the measurement. In addition, we can not distinguish between two non-orthogonal states with certainty, as we saw from the example in section 1.2.4.

This presents a problem as one of the key steps in a control scheme is measurement. For a quantum control scheme to be successful, we require the right type of measurement. In quantum control, destroying the state or projecting it onto another state will result in a loss of information contained in the state. If we can acquire information about a state after it has been perturbed by noise without disturbing it too much, we can correct it back to its initial state, allowing the information contained in the state to be preserved.

A weak measurement is a good choice of measurement; however, even with a weak measurement there will still be some influence on the system due to the measurement. By varying the strength of the measurement, we can control how much we disturb the system. If we make a measurement with minimum strength (no measurement) then there is no disturbance to the system; however, we do not gain any information about the state of the system. Increasing the measurement strength, we find that there is a trade-off between the amount of information one can gain about the state of

a system and the disturbance caused to the system. A measurement with maximum strength (a projective measurement), will maximally disturb the system and the probability of the result is strongly dependant on the previous state of the system. This behaviour leads us to believe that there will be an optimum measurement strength between the two extremes.

We need to find the optimal weak measurement which gives sufficient information about the system so that it can be controlled, while minimising the disturbance to the system.

1.4 Previous Work in Quantum Control

In this section, we will discuss a number of theoretical and experimental advances made in quantum control. Although the field of quantum control is in its infancy, the literature is by no means limited to the examples given in this brief summary. We will discuss a few of the pioneers in theoretical quantum control, some state-of-the-art experiments and a theoretical paper containing the idea of optimal measurements, which is also the theme of this thesis.

The pioneering theoretical work in quantum control was done in the 1980s by Belavkin, who formulated a complete mathematical theory of quantum mechanical feedback systems [7]. This was followed by the first papers in quantum optics discussing quantum limited feed back. Caves and Milburn [8] present a way to describe a continuous or 'dynamic' measurement of position then modify the basic model to include feedback to stabilise the position and momentum. Wiseman and Milburn were the first to explore the noise reducing capabilities of feedback in quantum optical systems [9]. The theory in [9] describes quantum-limited feedback of a homodyne current to control an optical cavity.

A theoretical proposal by Thomsen *et al.* [10] describes a technique for spin squeezing via coherent and continuous feedback. The scheme shows how one can prepare unconditional, or deterministically reproducible, spin squeezed states. The subsequent experiment was performed by Geremia *et al.* [11] where they used real-time feedback during a quantum non-demolition experiment of atomic spin-angular momentum.

Geremia *et al.* [12] recently showed that one can make sensitive measurements of the magnetic field, at the Heisenberg limit, using spin squeezing. In this paper, the uncertainty of one spin component is redistributed into the orthogonal spin component. It was shown that one can construct a Kalman filter[2] that optimally estimates the field magnitude from continuously observed conditional atomic dynamics.

[2]The Kalman filter is a set of mathematical equations that provides an efficient computational means to estimate the state of a process, in a way that minimises the mean of the squared error [13].

Smith *et al.* [14] used quantum feedback to suppress the oscillations of the electric field in an optical cavity. An atom in the cavity is coupled to a weak field. When a single photon escapes from the cavity, the oscillations of the valence electron of the atom increase, and after some time, these oscillations are transferred to the coupled field. The detection of the photon triggers a pulse which changes the driving frequency such that the oscillations of the field are suppressed for the duration of the pulse. When the pulse is turned off, the oscillations return with the same phase and amplitude information.

In a paper of particular interest in the context of this thesis, Doherty and Jacobs [15], discuss the theory behind measuring the position of an oscillator (for example, a trapped atom or a moving mirror forming one end of an optical cavity). In this paper, a laser incident on the oscillator results in a phase shift in the beam, allowing a continuous measurement of the position of the oscillator. By integrating the measurement signal it is possible to make an estimate of the position and momentum of the oscillator. Then on the basis of these estimates, it is possible to apply the appropriate force, proportional to the momentum, in the opposite direction to cool and confine the oscillator. In theme with the ideas within this thesis, high accuracy in the position measurement of a quantum system results in large variance in the momentum of that system. This means that in contrast with classical physics, quantum mechanically there will be an optimum measurement accuracy.

1.5 Thesis Structure

In this chapter, we covered some of the basic concepts of classical and quantum control. Chapter 2 introduces the formalisms that are used throughout this thesis. We begin with the qubit formalism used in quantum information when representing general quantum systems, then see how this ties in with the polarisation encoding formalism used in quantum optics where the quantum systems are no longer general, but single photons.

The quantum control proposal is discussed in Chapter 3, where we demonstrate how to model dephasing noise and the control system's behaviour. We then show how the quantum operations from Chapter 2 are used to perform the required measurements, feedback and correction.

Chapter 4 explores our scheme in comparison to doing nothing to the system and letting it evolve under dephasing noise. The quantum control scheme is also compared to a scheme where one discriminates between two possible states then replaces the states based on the results of the measurement. This discriminate-and-replace scheme is how one would go about correcting the states classically. The optimality of the quantum control scheme is also investigated.

In Chapter 5, we demonstrate how the proposed quantum control scheme could be implemented as a quantum optics experiment. We also explore which optical elements are required to build the quantum circuit, as well as discuss available sources and how the dephasing noise and feedback can be implemented experimentally.

1.6 Summary

Classical control plays an enormous role in modern technologies. Without feedback control, it would be nearly impossible to stabilise the systems required to build these technologies. We have already discussed how quantum systems break some of the assumptions behind classical control. The main point in this discussion is that a measurement of a quantum system necessarily disturbs it. Therefore, unlike in classical control, it is not always best to acquire as much information as possible about a quantum system.

Chapter 2

Formalism

In this chapter, we will cover the different formalisms used throughout this thesis. The chapter begins with how two-dimensional states can be represented and manipulated in the language of quantum information. We then introduce how to represent the quantum states by using the polarisation of a photon in optics. We also discuss how one can translate between these formalisms.

2.1 Qubit Formalism in Quantum Information

Classical computation and classical information revolve around the fundamental concept of a mathematical object called a *bit*[1]. A bit can be realised as a physical system with two distinct states, 0 or 1. In quantum computation and quantum information, we make use of the analogous *quantum bit* or the *qubit*. A qubit is a two-dimensional Hilbert space for a two level system. The system can be assigned the state $|0\rangle$ or $|1\rangle$, where $\{|0\rangle, |1\rangle\}$ is an orthonormal basis, which correspond to the classical states 0 and 1 [1]. An unusual property of the qubit is that it can also take on states which are in a *superposition* of $|0\rangle$ and $|1\rangle$, a phenomenon that is a characteristic of quantum physics. Such a state can be written as a *linear combination* of states:

$$|\psi\rangle \quad = \quad \alpha|0\rangle + \beta|1\rangle \tag{2.1}$$

where α and β are complex numbers. The state $|\psi\rangle$ is required to be a unit vector, $\langle\psi|\psi\rangle = 1$, therefore it is a requirement that $|\alpha|^2 + |\beta|^2 = 1$. This is often known as the *normalisation condition* for state vectors. We can also represent $|\psi\rangle$ in vector form as:

$$|\psi\rangle \quad = \quad \begin{bmatrix} \alpha \\ \beta \end{bmatrix} \qquad \text{or} \qquad \langle\psi| = [\alpha^* \quad \beta^*]\,. \tag{2.2}$$

[1] A *bit* is a *b*inary dig*it*.

Alternatively, we can represent a state $|\psi\rangle$ as a *density operator*:

$$\begin{aligned} \rho &= |\psi\rangle\langle\psi| && (2.3)\\ &= (\alpha|0\rangle + \beta|1\rangle)(\alpha^*\langle 0| + \beta^*\langle 1|) && (2.4)\\ &= |\alpha|^2|0\rangle\langle 0| + |\beta|^2|1\rangle\langle 1| + \alpha\beta^*|0\rangle\langle 1| + \alpha^*\beta|1\rangle\langle 0| && (2.5) \end{aligned}$$

or as a *density matrix*:

$$\rho = \begin{bmatrix} |\alpha|^2 & \alpha\beta^* \\ \alpha^*\beta & |\beta|^2 \end{bmatrix}. \quad (2.6)$$

If the state $|\psi\rangle$ is known with certainty, $\rho = |\psi\rangle\langle\psi|$ is said to be in a *pure state*, otherwise, it is said to be in a *mixed state* [1].

2.1.1 The Pauli Matrices

The *Pauli matrices* are 2×2 matrices that are often used in quantum information and quantum computation. They can be used to make transformation on states. The Pauli matrices are

$$\begin{aligned} I &= \begin{bmatrix} 1 & 0 \\ 0 & 1 \end{bmatrix} \qquad X = \begin{bmatrix} 0 & 1 \\ 1 & 0 \end{bmatrix} \\ Y &= \begin{bmatrix} 0 & -\mathrm{i} \\ \mathrm{i} & 0 \end{bmatrix} \qquad Z = \begin{bmatrix} 1 & 0 \\ 0 & -1 \end{bmatrix}. \end{aligned} \quad (2.7)$$

I is known as the *identity matrix* while X and Z are sometimes referred to as a *bit flip* and a *phase flip*, respectively. Y is equal to XZ, up to an overall, irrelevant phase, and can be thought of as both a *bit flip* and a *phase flip*. The Pauli matrices are Hermitian ($H^\dagger = H$) and unitary ($U^\dagger U = I$), which makes them useful in operator expansions.

Figure 2.1 shows the effect of the Pauli matrices on an arbitrary qubit state.

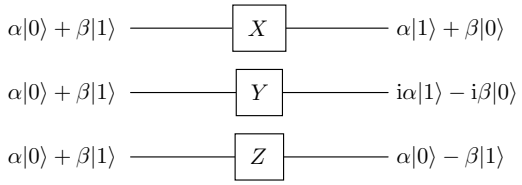

Figure 2.1: The Pauli matrix transformations on an arbitrary qubit state.

2.1.2 The Bloch Sphere

The *Bloch sphere* formalism provides a useful way in which to visualise the state of a single qubit. However it is limited as there is no simple generalisation of the sphere for multiple qubits [1]. The state in equation 2.1 can be rewritten as:

$$|\psi\rangle \quad = \quad \cos\tfrac{\theta}{2}|0\rangle + \mathrm{e}^{\mathrm{i}\varphi}\sin\tfrac{\theta}{2}|1\rangle \tag{2.8}$$

where θ and φ are real numbers which define a point on the three-dimensional Bloch sphere [1], as shown in figure 2.2. Pure states lie on the surface of the Bloch sphere and mixed states are found inside the sphere.

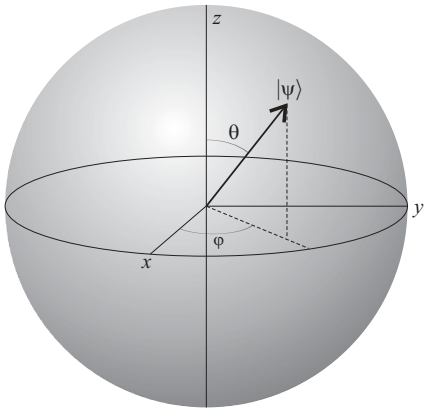

Figure 2.2: Bloch sphere representation of a qubit.

It is conventional to define a set of states which are eigenstates of X, Y, and Z, the axes of the Bloch sphere. The states at the poles of the sphere are $|0\rangle$ and $|1\rangle$, as shown in figure 2.3. The other states are linear combinations of these states:

$$|+\rangle \quad = \quad \frac{|0\rangle + |1\rangle}{\sqrt{2}} \tag{2.9}$$

$$|-\rangle \quad = \quad \frac{|0\rangle - |1\rangle}{\sqrt{2}} \tag{2.10}$$

$$|+\mathrm{i}\rangle \quad = \quad \frac{|0\rangle + \mathrm{i}|1\rangle}{\sqrt{2}} \tag{2.11}$$

$$|-\mathrm{i}\rangle \quad = \quad \frac{|0\rangle - \mathrm{i}|1\rangle}{\sqrt{2}}\,, \tag{2.12}$$

and are also shown in figure 2.3.

Any mixed state inside the sphere can be decomposed into a mixture of two pure states $|\psi\rangle$ and $|\phi\rangle$ on the surface of the sphere, such that the mixed state lies on a

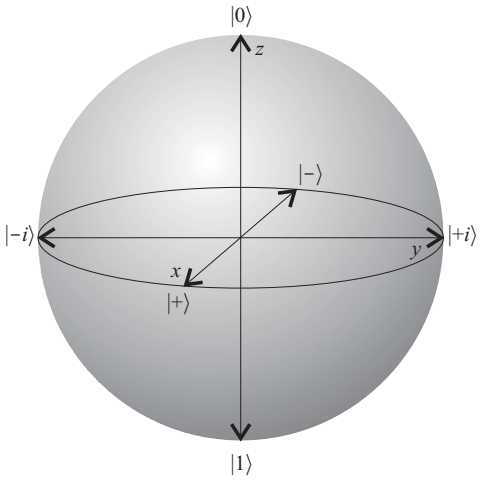

Figure 2.3: The six eigenstates of X, Y and Z, the axes of the Bloch sphere.

line joining the pure states:

$$\rho = p|\psi\rangle\langle\psi| + (1-p)|\phi\rangle\langle\phi| \tag{2.13}$$

where p is a coefficient which determines the weighting of each state. This is shown on a 2-d cross section of the Bloch sphere in figure 2.4. Furthermore, any mixed state on the inside of the sphere can be decomposed into pure states in an infinite number of ways.

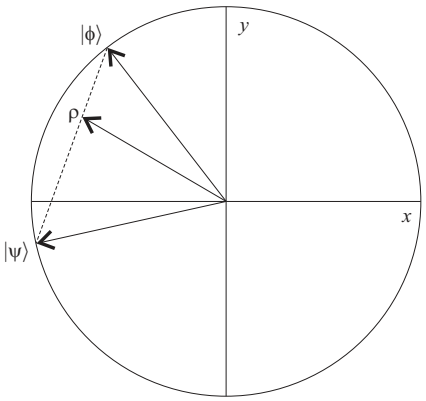

Figure 2.4: Any mixed state ρ inside the sphere can be decomposed into a mixture of two pure states $|\psi\rangle$ and $|\phi\rangle$ on the surface of the sphere.

If we know the density matrix ρ for a given state $|\psi\rangle$, we can calculate the Bloch sphere coordinates for that state.

$$x = \mathrm{Tr}\{\rho X\} \tag{2.14}$$
$$y = \mathrm{Tr}\{\rho Y\} \tag{2.15}$$
$$z = \mathrm{Tr}\{\rho Z\} \tag{2.16}$$

where $\vec{r} = (x, y, z)$ satisfies $||\vec{r}|| \leq 1$. Likewise, we can calculate ρ, given the real x, y and z coordinates:

$$\rho = \frac{I}{2} + \frac{1}{2}\Big(xX + yY + zZ\Big). \tag{2.17}$$

The completely mixed state $I/2$ is at the center of the sphere. Two states are orthogonal when they lie at opposite points on the sphere. For example, the states $|0\rangle$ and $|1\rangle$ are orthogonal, as are the states $|+\rangle$ and $|-\rangle$.

2.1.3 Single-Qubit Gates

The Pauli matrices can also be used to construct unitary *rotation operators*:

$$X_\theta = \mathrm{e}^{\mathrm{i}\theta X/2} = \cos\tfrac{\theta}{2} I + \mathrm{i}\sin\tfrac{\theta}{2} X = \begin{bmatrix} \cos\frac{\theta}{2} & \mathrm{i}\sin\frac{\theta}{2} \\ \mathrm{i}\sin\frac{\theta}{2} & \cos\frac{\theta}{2} \end{bmatrix} \tag{2.18}$$
$$Y_\theta = \mathrm{e}^{\mathrm{i}\theta Y/2} = \cos\tfrac{\theta}{2} I + \mathrm{i}\sin\tfrac{\theta}{2} Y = \begin{bmatrix} \cos\frac{\theta}{2} & \sin\frac{\theta}{2} \\ -\sin\frac{\theta}{2} & \cos\frac{\theta}{2} \end{bmatrix} \tag{2.19}$$
$$Z_\theta = \mathrm{e}^{\mathrm{i}\theta Z/2} = \cos\tfrac{\theta}{2} I + \mathrm{i}\sin\tfrac{\theta}{2} Z = \begin{bmatrix} \mathrm{e}^{+\mathrm{i}\theta/2} & 0 \\ 0 & \mathrm{e}^{-\mathrm{i}\theta/2} \end{bmatrix}. \tag{2.20}$$

These operators rotate the state by an angle θ about the x, y and z axes of the Bloch sphere.[2] Notice that Y_θ and Z_θ are Hermitian while X_θ is not.

2.1.4 Two-Qubit Gates

Apart from having gates which act on one qubit, there are also gates that act on two qubits.

In section 2.1.1, we introduced the Pauli-X matrix which acts on one qubit. The Pauli-X matrix is also known as the NOT gate and it takes $0 \to 1$ and $1 \to 0$. In this section we will introduce the controlled-NOT gate, or CNOT. The CNOT acts on two

[2] To avoid confusion, note that the Pauli matrices are X, Y and Z while the rotation matrices have subscripts which denote the angle of rotation X_θ, Y_θ and Z_θ.

qubits, one known as the *control* and the other as the *target*. If the control qubit is $|1\rangle$, the CNOT acts as a NOT gate on the target qubit and takes $|0\rangle \rightarrow |1\rangle$ and $|1\rangle \rightarrow |0\rangle$. If the control is $|0\rangle$, then the CNOT does nothing to the target qubit. We can represent the CNOT in matrix form as follows:

$$\text{CNOT} = \begin{bmatrix} 1 & 0 & 0 & 0 \\ 0 & 1 & 0 & 0 \\ 0 & 0 & 0 & 1 \\ 0 & 0 & 1 & 0 \end{bmatrix}. \tag{2.21}$$

The CNOT is written with respect to the amplitudes $|00\rangle$, $|01\rangle$, $|10\rangle$ and $|11\rangle$, in that order. Figure 2.5 shows how the CNOT acts on two qubits.

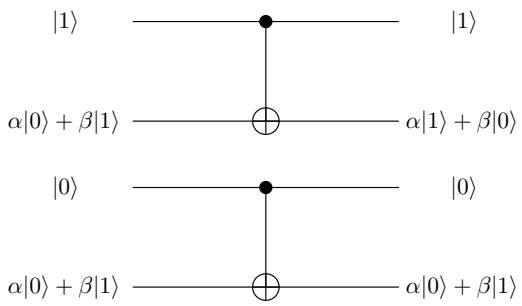

Figure 2.5: The CNOT gate acts like a NOT on the target ($\oplus$) qubit when the control ($\bullet$) qubit is in the state $|1\rangle$ and leaves the target qubit unchanged if the control qubit is $|0\rangle$

There exist other two-qubit gates. However, we are particularly interested in the CNOT as, together with local unitaries, it is universal and forms a building block of quantum circuits [1]. In addition, if the control is in a superposition state, the CNOT is entangling between the control and the target states.

2.2 General Transformations

The most general transformation on a single qubit state can be represented as a quantum operation:

$$\rho' = \mathcal{E}(\rho) = \sum_k E_k \rho E_k^\dagger \tag{2.22}$$

where the operation elements E_k satisfy the *completeness relation* $\sum_k E_k^\dagger E_k = I$, and are therefore *trace preserving*. $\mathcal{E}(\rho)$ takes the state ρ in the *input* Hilbert space $\mathcal{H}_{\text{in}}$ to the state ρ' in the *output* Hilbert space $\mathcal{H}_{\text{out}}$, and is called *positive* if it takes

a positive operator (an operator whose eigenvalues are non-negative) to a positive operator. The representation on the right of equation 2.22 is known as the *operator sum representation* [1].

It is sometimes beneficial to represent the transformation $\mathcal{E}$ by a positive, Hermitian operator K, in the following way.

If we know $\mathcal{E}(\rho)$, we can define K:

$$K = (I \otimes \mathcal{E})(|\psi^+\rangle\langle\psi^+|) \tag{2.23}$$

$$= \sum_k (I \otimes E_k)|\psi^+\rangle\langle\psi^+|(I \otimes E_k)^\dagger \tag{2.24}$$

where K acts on $\mathcal{H}_{\text{in}} \otimes \mathcal{H}_{\text{out}}$, $|\psi^+\rangle = \sum_j |j\rangle|j\rangle/\sqrt{d}$ and $|j\rangle$ is the basis. Likewise, if we know K, we can find $\mathcal{E}(\rho)$:

$$\mathcal{E}(\rho) = \text{Tr}_{\text{in}}\{(\rho^T \otimes I)K\}\,. \tag{2.25}$$

$\mathcal{E}$ is *completely positive* if it takes a positive operator to a positive operator while acting on a subspace of the density matrix. $\mathcal{E}$ and K contain the same information and if $\mathcal{E}$ is completely positive and trace preserving, then K must obey the following constraints [16, 17]:[3]

$$K \geq 0 \tag{2.26}$$

$$\text{Tr}_{\text{out}}\{K\} = I_{\text{in}}\,. \tag{2.27}$$

2.3 Polarisation Encoding in Optics

One method of encoding a photonic qubit is to use two orthogonal polarisations of a single photon. We can represent a photonic qubit on the *Poincaré sphere* (see figure 2.6), the polarisation equivalent of the Bloch sphere. Table 2.1 shows how the states on the Poincaré sphere are equivalent to the states on the Bloch sphere.

The Poincaré sphere is analogous to the Bloch sphere, however a different convention is used in optics where right (R) and left (L) circular polarisations are placed at the poles of the Poincaré sphere. This means that the R-L axis actually corresponds to the y axis on the Bloch sphere. If we compare the sphere in figure 2.6 to the sphere in figure 2.3, we see that the y and z axes have been swapped, however, this is only a matter of convention.

Single photon qubits are well defined and since, at optical frequencies, the environment is a vacuum the qubits are decoupled from the environment. If the qubits are

[3] A clear and concise discussion of this is presented in [18].

Bloch sphere	Poincaré sphere
$\|0\rangle$	$\|H\rangle$ horizontal polarisation
$\|1\rangle$	$\|V\rangle$ vertical polarisation
$\|+\rangle$	$\|D\rangle$ diagonal polarisation
$\|-\rangle$	$\|A\rangle$ anti-diagonal polarisation
$\|+\mathrm{i}\rangle$	$\|R\rangle$ right circular polarisation
$\|-\mathrm{i}\rangle$	$\|L\rangle$ left circular polarisation

Table 2.1: The states on the Bloch sphere can be written as equivalent states on the Poincaré sphere.

encoded in polarisation, then all single qubit gates can be done with passive, linear optics, for example, wave plates. It is still difficult to construct two qubit gates in optics, however this can be done non-deterministically and has been demonstrated by a number of groups [4, 19, 20, 21, 22]. Therefore, we have chosen to propose our quantum control scheme to be implemented with single photons, as the tools required for our scheme are already well developed in optics. In the rest of this section we will outline the optical elements required to construct the gates introduced in the previous section.

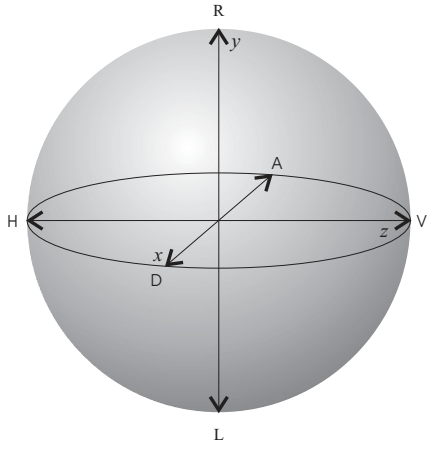

Figure 2.6: Different polarisations of light can be represented on the Poincaré sphere. The six eigenstates of X, Y and Z are horizontal (H), vertical (V), diagonal (D), anti-diagonal (A), right (R) and left (L) circular polarisations.

2.3.1 Beamsplitters

A *beamsplitter* is a partially reflective optical element which reflects some of the incident light and transmits the rest (assuming no absorption). The amount of light reflected is represented by the intensity reflection coefficient ϵ. Consider the beamsplitter shown in figure 2.7.

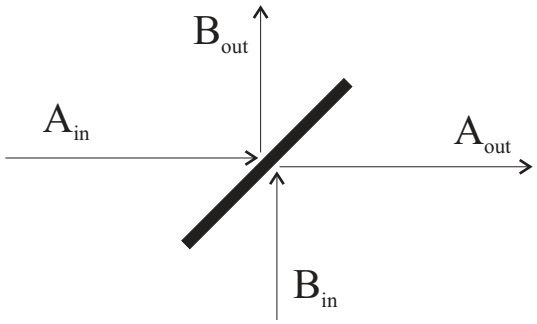

Figure 2.7: Conceptual diagram of a beam splitter. A_{in} and B_{in} represent the input modes while A_{out} and B_{out} represent the output modes.

In quantum mechanics, we assume that the input beams are travelling beams described by the operators A_{in} and B_{in}. The beam splitter can be simply described by a transformation from the two *input* mode operators into two *output* mode operators A_{out} and B_{out} [23]:

$$\begin{bmatrix} B_{\text{out}} \\ A_{\text{out}} \end{bmatrix} = \begin{bmatrix} \sqrt{\epsilon} & \sqrt{1-\epsilon} \\ -\sqrt{1-\epsilon} & \sqrt{\epsilon} \end{bmatrix} \begin{bmatrix} A_{\text{in}} \\ B_{\text{in}} \end{bmatrix}. \tag{2.28}$$

The '$-$' sign comes from the choice of beamsplitter convention. The usual choice is to set three relative phases to zero and the fourth to π. The normal explanation is that one of the reflected waves has a phase shift of 180° with respect to all other waves [23], which is one choice of phase convention that satisfies conservation of energy. It is not difficult to see that for $\epsilon = 1$ and $\epsilon = 0$, the output modes are

$$\begin{bmatrix} B_{\text{out}} \\ A_{\text{out}} \end{bmatrix} = \begin{bmatrix} A_{\text{in}} \\ B_{\text{in}} \end{bmatrix} \qquad \text{and} \qquad \begin{bmatrix} B_{\text{out}} \\ A_{\text{out}} \end{bmatrix} = \begin{bmatrix} B_{\text{in}} \\ -A_{\text{in}} \end{bmatrix} \tag{2.29}$$

respectively.

The beamsplitter turns out to be equivalent to a Y_θ rotation:

$$B(\theta) \equiv Y_\theta = \mathrm{e}^{\mathrm{i}\theta Y/2} = \begin{bmatrix} \cos\frac{\theta}{2} & \sin\frac{\theta}{2} \\ -\sin\frac{\theta}{2} & \cos\frac{\theta}{2} \end{bmatrix}. \tag{2.30}$$

Again, it is not difficult to see that for $\theta = 0$ and $\theta = \pi$, the output modes are the same as in equations 2.29. When $\theta = \pi/2$, the output will be an equal superposition of A_{in} and B_{in}, corresponding to a 50/50 ($\epsilon = 1/2$) beam splitter .

2.3.2 Wave Plates

Experimentalists can make qubits in the lab in the form of polarisation-encoded photons. They manipulate the photons using wave plates. There is no optical element which will apply a transformation like the matrices introduced in section 2.1, however, it is possible to construct such rotations by arranging a series of wave plates in a particular order. The most common wave plates are quarter-wave plates (QWP) and half-wave plates (HWP). One can align the optical axis of the wave plate with one of the axes on the linear polarisation circle of the Poincaré sphere. The HPW and QWP rotate the states on the sphere about the optical axis by 90° and 180° respectively. The following matrix representations of the wave plates assume that the optical axis is the $H - V$ axis.

$$\mathrm{Q} = \begin{bmatrix} 1 & 0 \\ 0 & -\mathrm{i} \end{bmatrix} \tag{2.31}$$

$$\mathrm{H} = \begin{bmatrix} 1 & 0 \\ 0 & -1 \end{bmatrix}. \tag{2.32}$$

However, we can rotate the optical axis parallel to any linear polarisation (anywhere on the equator). The wave plate operations can be generalised to three steps [24]: first apply a rotation about the R-L axis by some angle ϕ; then apply a wave plate; and then apply another rotation by some angle $-\phi$:

$$\mathrm{Q}(\phi) = R(-\phi)\ \mathrm{Q}\ R(\phi) \tag{2.33}$$

$$\mathrm{H}(\phi) = R(-\phi)\ \mathrm{H}\ R(\phi)\,. \tag{2.34}$$

Armed with these general wave plate operations, we can construct the rotations from section 2.1:

$$X_\theta = \mathrm{Q}(0)\ \mathrm{H}(\tfrac{-\theta}{2})\ \mathrm{Q}(0) = \begin{bmatrix} \cos\frac{\theta}{2} & \mathrm{i}\sin\frac{\theta}{2} \\ \mathrm{i}\sin\frac{\theta}{2} & \cos\frac{\theta}{2} \end{bmatrix} \tag{2.35}$$

$$Y_\theta = \mathrm{H}(\tfrac{-\theta-\pi}{4})\ \mathrm{H}(\tfrac{\theta-\pi}{4}) = \begin{bmatrix} \cos\frac{\theta}{2} & \sin\frac{\theta}{2} \\ -\sin\frac{\theta}{2} & \cos\frac{\theta}{2} \end{bmatrix} \tag{2.36}$$

$$Z_\theta = \mathrm{Q}(\tfrac{\pi}{2})\ \mathrm{H}(\tfrac{\pi+\theta}{2})\ \mathrm{Q}(\tfrac{\pi}{2}) = \begin{bmatrix} \mathrm{e}^{+\mathrm{i}\theta/2} & 0 \\ 0 & \mathrm{e}^{-\mathrm{i}\theta/2} \end{bmatrix}. \tag{2.37}$$

We want to implement our quantum control scheme experimentally in optics. The

states will be encoded in the polarisation of single photons, and beam splitters and wave plates will be used to construct the required one and two qubit gates. This is discussed in chapter 5.

2.4 Summary

Throughout this thesis, we will make use of mainly two types of formalisms: the qubit formalism used in quantum information; and the polarisation encoding formalism used in quantum optics. In the qubit formalism, we make use of the Bloch sphere as a way of visually representing a single qubit. Qubits are an abstraction that allows for a generic description of the states quantum systems. In optics, we can represent a single qubit using the orthogonal polarisations of a single photon and all single qubit rotations can be implemented by a number of half and quarter-wave plates.

We will use the qubit formalism to present and analyse the quantum control scheme and then translate the scheme to the polarisation encoding formalism when we propose the prototype optics experiment.

Chapter 3

Quantum Control Proposal

This chapter introduces the quantum control scheme. We describe how we can model the system and noise using the quantum information formalism introduced in the previous chapter.

Consider a system that encounters some noise and its state is perturbed. If the state of the system before the noise is known, we do not need to correct the noisy system, we can simply reprepare the system in the original state. A procedure that truly demonstrates quantum control must necessarily function on two or more possible states that cannot be easily distinguished.

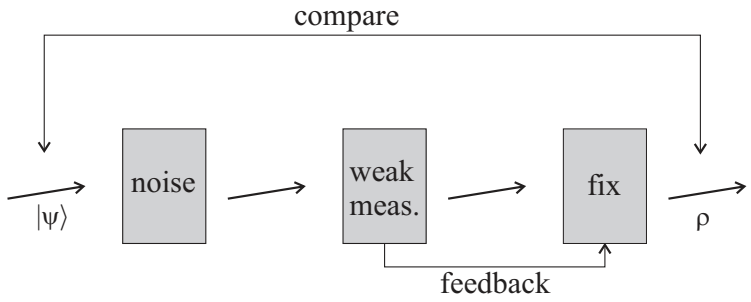

Figure 3.1: Conceptual diagram of the quantum control procedure. The state (represented by an arrow) $|\psi\rangle$ goes through some noise, gets measured using a weak measurement and then is corrected based on the results of the weak measurement. The output state ρ is compared with the input state $|\psi\rangle$ to characterise how well the scheme works.

We propose a scheme which reduces the effects of noise, through a feedback control procedure, on a system that can be prepared in one of two possible states. Consider two parties, Alice and Bob. Alice wants to send a series of systems, each prepared in one of two non-orthogonal states to Bob. These non-orthogonal states can be used to demonstrate the use of our scheme, because there is no way that two non-orthogonal states can be precisely distinguished by measurement. If the states were

orthogonal, the scheme would be unnecessary, as it would be possible to distinguish the states, by using a measurement in the basis constructed out of the orthogonal states to be distinguished, and replace them.

This approach uses classical control concepts and we can use it to attempt to distinguish the two non-orthogonal states and then reprepare the state based on the results. This will work to some degree but is not necessarily the best possible approach. The quantum approach is to do the opposite and *not* distinguish the states. If we can find out how the state was perturbed, then we can correct it without actually knowing which state the system was in to begin with.

When Alice sends one of the states to Bob, the state will decohere as it passes through a noisy channel. Bob will use the QND scheme described to perform a weak measurement on the state. He will then attempt to correct the system to its original state based on the measurement results. The performance of the quantum control scheme can be characterised by comparing Bob's state with Alice's original. A conceptual diagram for this procedure is shown in figure 3.1.

The scheme we are proposing is shown in figure 3.2. We will explain the scheme in detail in the following sections.

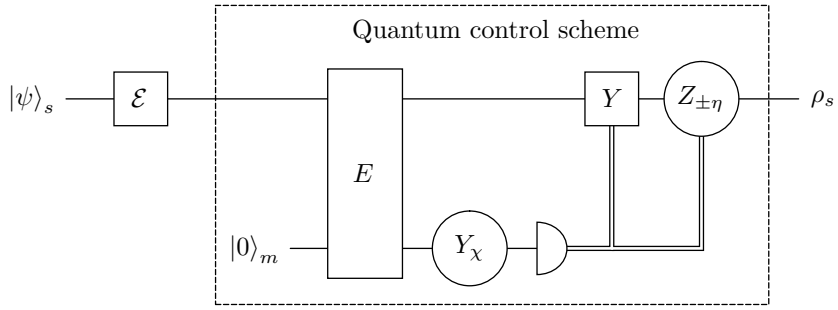

Figure 3.2: Circuit diagram of the quantum control proposal. The signal state $|\psi\rangle_s$ is sent through a noisy channel $\mathcal{E}$. The quantum control scheme consists of everything inside the dashed box: The noisy signal state ρ_s and the meter state $|0\rangle_m$ are entangled using the entangling gate E, the strength of the measurement is set using the rotation Y_χ and the meter state is measured. Based on the measurement results, we either apply a Y to the signal state and then a rotation $Z_{-\eta}$ or we skip the Y and go straight to the rotation Z_η which corrects the signal state.

3.1 Initial Input States

As discussed previously, Alice will randomly send one of two non orthogonal states to Bob. These states are required to be non-orthogonal so that they can not be

distinguished with certainty. To ensure non-orthogonality between states, the inner product of the states must be non-zero. The two states that Alice will prepare are:

$$|\psi_1\rangle_s = \cos\tfrac{\theta}{2}|+\rangle + \sin\tfrac{\theta}{2}|-\rangle \quad (3.1)$$

$$|\psi_2\rangle_s = \cos\tfrac{\theta}{2}|+\rangle - \sin\tfrac{\theta}{2}|-\rangle \quad (3.2)$$

where $|\pm\rangle = (|0\rangle \pm |1\rangle)/\sqrt{2}$ and θ is an angle on the Bloch sphere, as shown in figure 3.3. The subscript s denotes that this is the system state (as opposed to the meter). Any two states can be expressed in this form, with the right form of Bloch sphere coordinates, for example $|\phi\rangle = \sin\theta/2|0\rangle \pm \cos\theta/2|1\rangle$. The inner product between $|\psi_1\rangle_s$ and $|\psi_2\rangle_s$ is

$$\begin{aligned} {}_s\langle\psi_1|\psi_2\rangle_s &= (\cos\tfrac{\theta}{2}\langle+| + \sin\tfrac{\theta}{2}\langle-|)(\cos\tfrac{\theta}{2}|+\rangle + \sin\tfrac{\theta}{2}|-\rangle) && (3.3)\\ &= \cos^2\tfrac{\theta}{2} - \sin^2\tfrac{\theta}{2} && (3.4)\\ &= \cos\theta && (3.5) \end{aligned}$$

which is nonzero except when $\theta = \pi/2$. The angle θ determines the orthogonality between the states. From figure 3.3, we can see that this is what would be expected, as an angle of $\theta = \pi/2$ puts the states along the z axis. We have chosen the states to lie on the x-z plane for reasons which will become apparent when we discuss the noise model and measurement techniques later in this chapter.

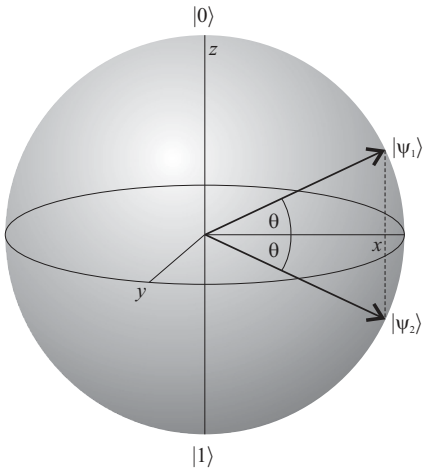

Figure 3.3: The initial states $|\psi_1\rangle_s$ and $|\psi_2\rangle_s$. Alice will send one of these states to Bob.

The signal states can be represented as density matrices, $\rho_{s1} = |\psi_1\rangle_s\langle\psi_1|$ and $\rho_{s2} = |\psi_2\rangle_s\langle\psi_2|$, respectively. As Alice will randomly send either ρ_{s1} or ρ_{s2}, the

state of the signal can be represented as an equal mixture of the two states,

$$\rho_s = \tfrac{1}{2}\rho_{s1} + \tfrac{1}{2}\rho_{s2}. \tag{3.6}$$

The density matrix ρ_s is the description of the state for someone who does not know which state Alice chooses, as it takes both possible states into consideration.

3.2 Dephasing Noise

As a system propagates, it will necessarily be affected by noise. We have chosen to use dephasing (defined below) as a simple model of this noise. Dephasing noise commonly occurs in physical systems, for example a photon propagating through an optical fibre experiences dephasing.

Mathematically, we can think of the dephasing noise as applying a phase flip on the state with some probability p and doing nothing to the state with probability $(1-p)$. The quantum operation that is implemented by this noise process is:

$$\mathcal{E}(\rho) \;=\; p(Z\rho Z) + (1-p)\rho\,. \tag{3.7}$$

Our goal is to pass our system of two non-orthogonal states through the noise, then try to control the system. In the previous section, we chose to prepare the non-orthogonal states symmetric about the equator. This is the best way to prepare two non-orthogonal states for this scheme as the dephasing noise acts in a way that allows a measurement of the effect of the noise without gaining any information about the state of the system.

To gain an intuitive understanding of what effect the noise has on a state, let us first consider a state $|+\rangle$ along the x axis (see figure 3.4). We will define the density matrix for this state as $\sigma = |+\rangle\langle+|$. In this example we will make the probability of a phase flip $p = 1/4$. This means that 25% of the time, the state will be flipped and 75% of the time, the state will remain unchanged. Using equation 3.7 and the vector representation from equation 2.17,

$$\begin{aligned}
\mathcal{E}(\sigma) &= \tfrac{1}{4}(Z\sigma Z) + \tfrac{3}{4}\sigma \\
&= \tfrac{1}{4}Z(\tfrac{I}{2} + \tfrac{1}{2}X)Z + \tfrac{3}{4}(\tfrac{I}{2} + \tfrac{1}{2}X) \\
&= \tfrac{1}{4}(\tfrac{I}{2} - \tfrac{1}{2}X) + \tfrac{3}{4}(\tfrac{I}{2} + \tfrac{1}{2}X) \\
&= \tfrac{I}{2} + \tfrac{1}{4}X \\
&= \tfrac{I}{2} + \tfrac{1}{2}x'X
\end{aligned}$$

where the new component along the x axis is $x' = 1/2$.

From figure 3.4, we can see that this results in the state being shortened along the x axis by a factor of $1/2$.

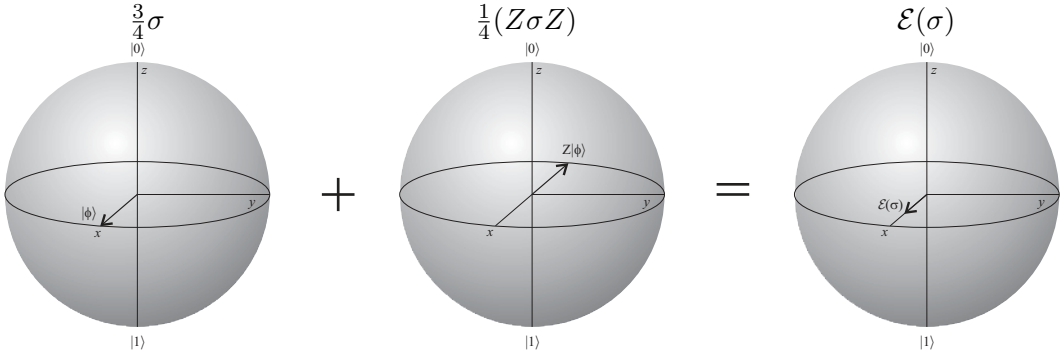

Figure 3.4: Decomposition of the dephasing noise into $\mathcal{E}(\sigma) = p(Z\sigma Z) + (1-p)\sigma$, for $p = 3/4$.

An equivalent way to describe the noise process is a rotation of the state about the z axis by some angle α half of the time, and a rotation of the state about the z axis by some angle $-\alpha$ the remaining half of the time. The angle α is related to the probability p such that $p = \sin^2(\alpha/2)$. It is easier to follow the derivation which proves this if we work backwards.

$$\begin{aligned}
\mathcal{E}(\rho) &= \tfrac{1}{2}Z_\alpha \rho Z_\alpha^\dagger + \tfrac{1}{2}Z_{-\alpha}\rho Z_{-\alpha}^\dagger \\
&= \tfrac{1}{2}\mathrm{e}^{\mathrm{i}\alpha Z/2}\rho\mathrm{e}^{-\mathrm{i}\alpha Z/2} + \tfrac{1}{2}\mathrm{e}^{-\mathrm{i}\alpha Z/2}\rho\mathrm{e}^{\mathrm{i}\alpha Z/2} \\
&= \tfrac{1}{2}\Big(\cos\tfrac{\alpha}{2}I + \mathrm{i}\sin\tfrac{\alpha}{2}Z\Big)\rho\Big(\cos\tfrac{\alpha}{2}I - \mathrm{i}\sin\tfrac{\alpha}{2}Z\Big) \\
&\quad + \tfrac{1}{2}\Big(\cos\tfrac{\alpha}{2}I - \mathrm{i}\sin\tfrac{\alpha}{2}Z\Big)\rho\Big(\cos\tfrac{\alpha}{2}I + \mathrm{i}\sin\tfrac{\alpha}{2}Z\Big) \\
&= \sin^2\tfrac{\alpha}{2}Z\rho Z + \cos^2\tfrac{\alpha}{2}\rho
\end{aligned}$$

If we now substitute $\sin^2(\alpha/2) = p$ then we get

$$\mathcal{E}(\rho) = p(Z\rho Z) + (1-p)\rho$$

Figure 3.5 shows that this alternate way describing the dephasing noise produces the same result as in figure 3.4. In this example, $\alpha = \pi/3$ which corresponds to $p = 1/4$.

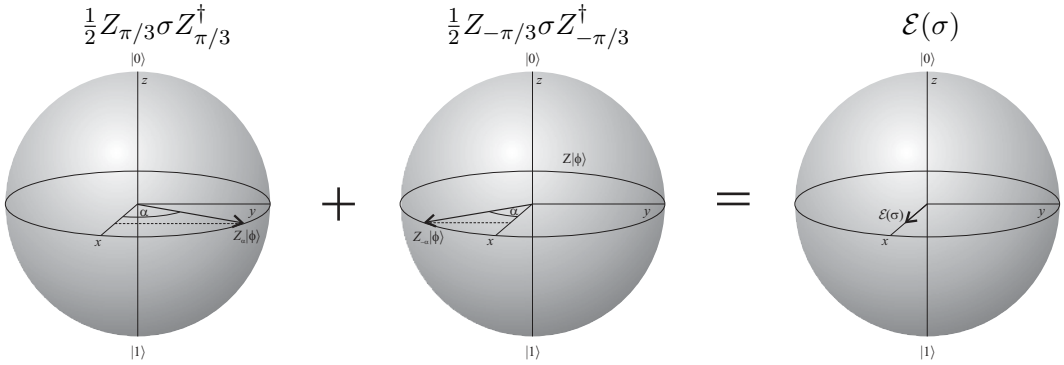

Figure 3.5: Decomposition of the dephasing noise into $\mathcal{E}(\sigma) = \frac{1}{2}Z_{\alpha}\sigma Z^{\dagger}_{\alpha} + \frac{1}{2}Z_{-\alpha}\sigma Z^{\dagger}_{-\alpha}$, for $\alpha = \pi/3$.

For a more general state $|\psi\rangle$, the noise has the effect of shortening the state along the x axis of the Bloch sphere while leaving the z component of the state unchanged, as is shown in figure 3.6.

Figure 3.7 shows what the dephasing noise of $p = 0.3$ does to every state on the surface of the Bloch sphere. The z component of the states remains unchanged, while the x and y components get shortened by a factor of $1 - 2p$ [1].

The effect of the dephasing noise on the two possible input states is to shorten the states along the x axis by the same amount, while keeping the Euclidean distance between the states the same — that is, keeping the straight line between the points on the Bloch sphere the same.

3.3 Measurement

In this section, we will introduce the quantum control scheme. In Chapter 1, we determined that making a weak measurement on the signal system enables one to perform feedback control on the system, based on the results of this measurement. The quantum operation used to perform this type of measurement is an entangling gate E (see figure 3.8) which sets up correlations between the signal state and the meter state.

In chapter 1, we discussed the use of a controlled-NOT (CNOT) gate and an ancillary meter state to perform weak measurements on the signal state. We will prepare the meter system in the state:

$$|\psi\rangle_m = |0\rangle_m \,. \tag{3.8}$$

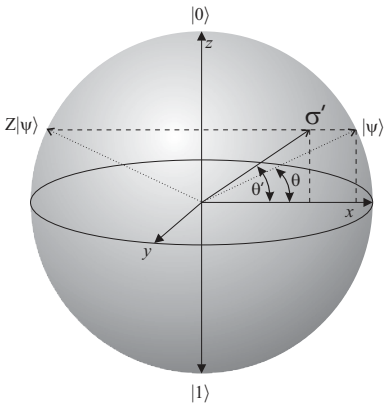

Figure 3.6: Bloch sphere representation of the effect of dephasing noise on a state $|\psi\rangle$. The noise has the effect of shortening the state along the x axis of the Bloch sphere while leaving the z component of the state unchanged. θ is the original angle on the Bloch sphere. When the state is shortened, the angle becomes θ'. Notice that the viewing angle has been rotated from the viewing angle used in previous figures.

Returning to the scenario from the beginning of this chapter: Alice will randomly select either $|\psi_1\rangle$ or $|\psi_2\rangle$ to send to Bob. The dephasing noise can be thought of as rotating the state she sends about the z axis by α and $-\alpha$. We assume that the dephasing channel has been previously characterised and we know what α is. In our quantum control scheme, we do not want to gain information about which of the states she sent. In fact, we want to avoid acquiring this information, but nevertheless we want to determine the effect of the noise.

If we think of the noise in terms of rotations, then in a way, the scheme works by gaining information about which way the noise rotated the state about the z axis. The noise has the same effect on both states, rotating them such that the y component is the same in each state. By making a measurement along the y axis, we can gain maximal information about the noise and no information about which state the signal was in. A detector is used to measures the state of the meter system, giving the result 0 or 1 depending on which state it measures.

If the meter state is measured immediately after entanglement, we perform a completely projective measurement on the signal state. However, if we add a rotation on the meter state about the y axis by an angle χ, we can vary the strength of the measurement.

When $\chi = 0$, there is no rotation and the measurement remains projective, projecting the state onto either $|+\mathrm{i}\rangle$ or $|-\mathrm{i}\rangle$. As χ increases, the measurement becomes weaker: the signal state is still rotated about the z axis, lengthened and brought closer to the equator, but not as much as for a projective measurement. One can

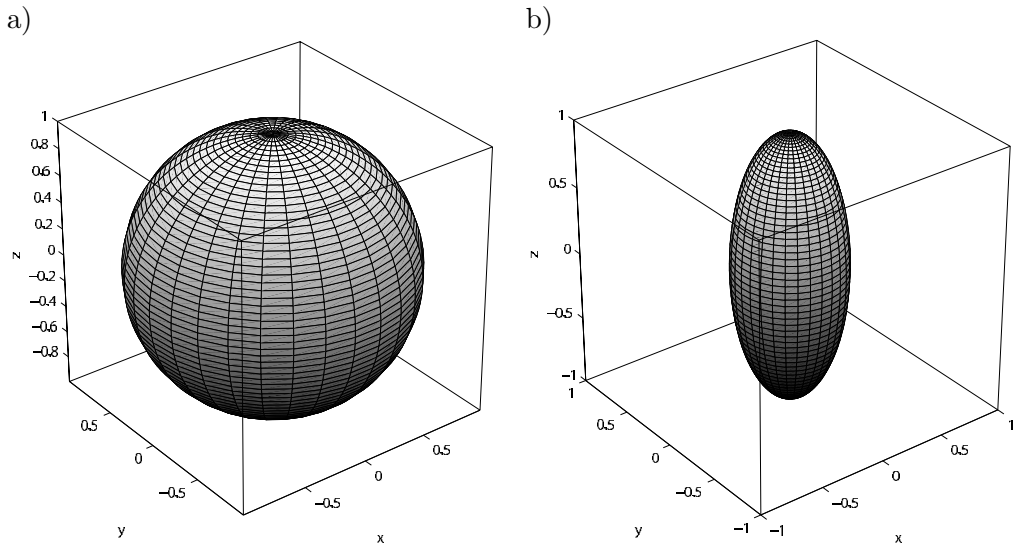

Figure 3.7: a) All states on the surface of the Bloch sphere before noise and b) all states after noise ($p = 0.3$). The dephasing noise leaves the z component of the states unchanged while shortening the x and y components of the states by a factor of $1 - 2p$ [1].

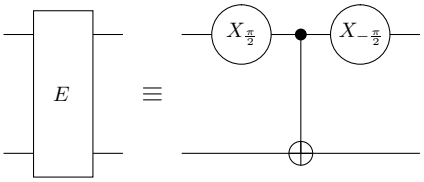

Figure 3.8: The entangling gate used to set up correlations between the signal and meter states.

think of this as 'partially projecting' the state. At $\chi = \pi/2$, there is no measurement and the signal state is unaffected. This is shown in figure 3.9.

To ensure that the final state is as similar to the initial state as possible, the final state should be as pure as possible and the angle from the equator should be as similar as possible to the initial angle θ. The stronger the measurement, the longer, and therefore more pure, the state becomes. However, the state also becomes closer to the equatorial plane. There is an optimal measurement strength which optimises the trade-off between the pureness and the position of the state.

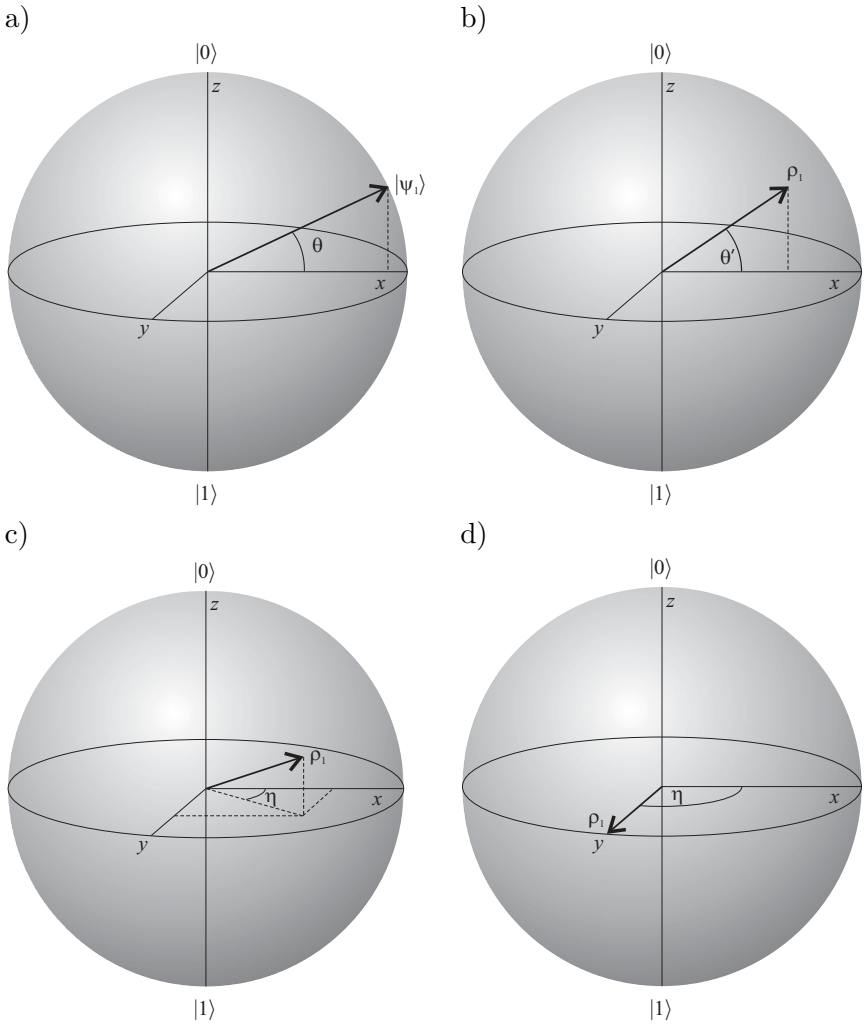

Figure 3.9: Bloch sphere representation of the effect on the signal state by a measurement of the meter state. The measurement shown here yields the result 0. For measurements yielding the result 1, the behaviour would be symmetric in the x-z plane. a) The state before noise; and b) the state after noise. The state also looks like this when $\chi = \frac{\pi}{2}$ and no measurement is made. c) $0 < \chi < \frac{\pi}{2}$. A weak measurement partially projects the state into $|-\mathrm{i}\rangle$ d) $\chi = 0$. A strong measurement complectly projects the state into $|-\mathrm{i}\rangle$.

3.3.1 Example of a Weak Measurement

Let us consider a simpler example by working in the $\{|0\rangle, |1\rangle\}$ basis. If we have a signal system in the state $|\phi\rangle_s = \alpha|0\rangle_s + \beta|1\rangle_s$ and the meter system in the state $|\phi\rangle_m = |0\rangle_m$, they can be entangled using the CNOT. Writing the combined signal-meter state in vector form:

$$|\phi_{\text{in}}\rangle_{sm} = \alpha|0\rangle_s|0\rangle_m + \beta|1\rangle_s|0\rangle_m = \begin{bmatrix} \alpha \\ 0 \\ \beta \\ 0 \end{bmatrix} \tag{3.9}$$

and applying the CNOT, we get:

$$|\phi_{\text{out}}\rangle_{sm} = \begin{bmatrix} 1 & 0 & 0 & 0 \\ 0 & 1 & 0 & 0 \\ 0 & 0 & 0 & 1 \\ 0 & 0 & 1 & 0 \end{bmatrix} \begin{bmatrix} \alpha \\ 0 \\ \beta \\ 0 \end{bmatrix} = \begin{bmatrix} \alpha \\ 0 \\ 0 \\ \beta \end{bmatrix} = \alpha|0\rangle_s|0\rangle_m + \beta|1\rangle_s|1\rangle_m\,. \tag{3.10}$$

At this point, a Y_χ rotation to determine the measurement strength would be applied, but since we want to first consider the case where a strong measurement ($\chi = 0$) is made, the rotation simplifies to a 4×4 identity matrix. Measuring the state in the $\{|0\rangle, |1\rangle\}$ basis, results in a projective measurement that projects the signal state into $|0\rangle$ when the measurement of the meter state yields the result 0, and projects the signal state into $|1\rangle$ when the measurement yields the result 1.

At the other extreme, to make the weakest measurement (no measurement), a $Y_{\pi/2}$ rotation is applied to the meter state after entanglement.

$$\begin{aligned} |\phi_{\text{out}}\rangle_{sm} &= \frac{1}{\sqrt{2}} \begin{bmatrix} 1 & 1 & 0 & 0 \\ -1 & 1 & 0 & 0 \\ 0 & 0 & 1 & 1 \\ 0 & 0 & -1 & 1 \end{bmatrix} \begin{bmatrix} \alpha \\ 0 \\ 0 \\ \beta \end{bmatrix} \\ &= \frac{1}{\sqrt{2}} \begin{bmatrix} \alpha \\ -\alpha \\ \beta \\ \beta \end{bmatrix} = \frac{\alpha|0\rangle_s + \beta|1\rangle_s}{\sqrt{2}}|0\rangle_m - \frac{\alpha|0\rangle_s - \beta|1\rangle_s}{\sqrt{2}}|1\rangle_m\,. \end{aligned} \tag{3.11}$$

If a measurement of the meter gives the result 0, then the signal will be in the state $(\alpha|0\rangle + \beta|1\rangle)/\sqrt{2}$. However, if the measurement gives the result 1, a phase flip needs to be applied to the signal state, which then also results in the signal being in the state $(\alpha|0\rangle + \beta|1\rangle)/\sqrt{2}$. As expected, no measurement of the meter state gives no information about the state of the signal. One can imagine that when χ is

somewhere between 0 and $\pi/2$, there will be some, but not total, measurement and some, but not total, 'projection'.

In the quantum controls scheme, where the states are represented in the $\{|+\rangle, |-\rangle\}$ basis, one can construct an equivalent but slightly messier argument. This introduces two minor changes to the process: a Pauli-Y operation is applied to the signal state (instead of a phase flip) when a measurement of the meter state gives the result 1; and two $X_{\pm\theta}$ rotations need to be applied to the signal state, before and after the CNOT.

3.4 Correction

After the measurement strength is determined by applying Y_χ, the density matrix for the signal state is

$$\rho_s = \begin{bmatrix} \frac{1}{2}(1+\sin\theta\sin\chi) & \frac{1}{2}(\cos\chi\sin\eta \\ & +(1-2p)\cos\eta\cos\theta\sin\chi) \\ \frac{1}{2}(\cos\chi\sin\eta & \\ +(1-2p)\cos\eta\cos\theta\sin\chi) & \frac{1}{2}(1-\sin\theta\sin\chi) \end{bmatrix}. \quad (3.12)$$

The last step in the procedure is to correct the state based on the result of the measurement. The state is corrected by rotating it about the z axis on the Bloch sphere by an angle η. Depending on whether the measurement result was 1 or 0, the state will be rotated either left or right. We can see from figure 3.9 that the angle of rotation η is

$$\tan\eta = \frac{y}{x}\,. \quad (3.13)$$

We can calculate x and y from the density matrix in equation 3.12 using equations 2.14 and 2.15:

$$x = (1-2p)\cos\theta\sin\chi \quad (3.14)$$

$$y = \cos\chi\,. \quad (3.15)$$

This gives an equation for η in terms of the noise p, the angle on the Bloch sphere θ and the measurement strength χ:

$$\tan\eta = \frac{1}{(1-2p)\cos\theta\tan\chi}\,. \quad (3.16)$$

We can calculate η, because we have previously characterised the dephasing noise. When we perform the experiment, we only need to determine if the angle of rotation was $+\eta$ or $-\eta$. Figure 3.10 shows what the state looks like after a measurement that

yields the result 0 and after the state is corrected by rotating it about the z axis of the Bloch sphere by an angle η. The corrected state in figure 3.10 b) may at first look very much like the noisy state, before measurement and correction, in figure 3.9 b) but the corrected state is in fact more pure and closer to the original state than the noisy state.

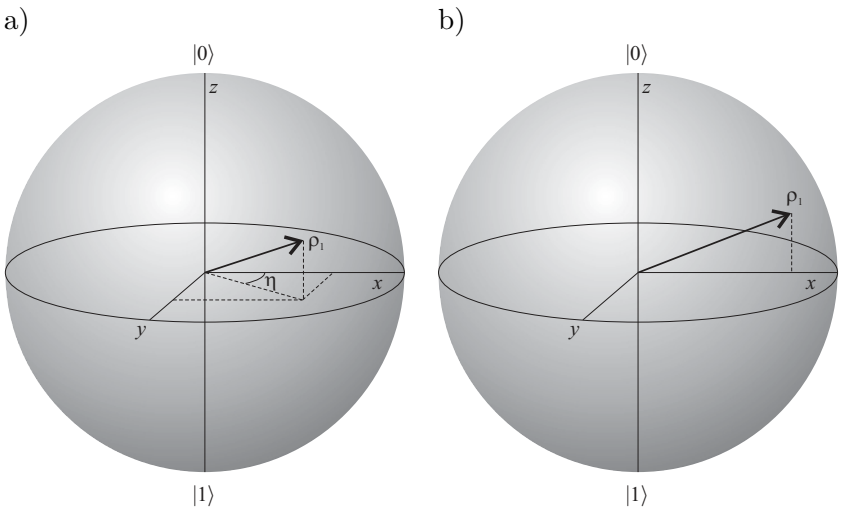

Figure 3.10: Bloch sphere representation of the state a) after measurement and b) after correction. Notice that the sphere in part a) is the same as the sphere in figure 3.9 c).

3.5 Summary

In this chapter, we discussed the proposed quantum control scheme. One of two possible non-orthogonal states is sent from one party to another. The possible states are required to be non-orthogonal to demonstrate the need for a quantum control scheme. After being sent, the states will inevitably encounter noise which we have modelled as dephasing noise.

The key thing about the quantum control scheme is that it relies on acquiring information about the effect of the noise rather than learning anything about the state of the system. We make use of an ancillary meter state by entangling it with a signal state and performing a weak measurement by measuring the meter state. We can correct the signal state, based on the information gained from this measurement which tells us about how the signal state was perturbed.

To characterise how well our quantum control scheme works, we want to compare the corrected output state in figure 3.10 b) with the initial input state in figure 3.9 a). This will be the topic of the next chapter.

Chapter 4

Performance and Characterisation

To characterise how well our scheme performs at controlling the state, we need to compare the measured and corrected state with the initial input signal state. One way that this can be done is by calculating the *fidelity* between the two states. The fidelity is a measure that determines how similar two quantum systems are [1]. We use the fidelity to see how well our scheme performs when compared with two scenarios: the state is sent through the noisy channel and we do not attempt to measure or correct it at all; and the state is sent through the noisy channel and we correct it using a classical-like discriminate-and-replace technique. We also investigate the optimality of the quantum control scheme.

4.1 Fidelity and its Properties

The fidelity between two states ρ and σ is defined to be:

$$F(\rho,\sigma) = \left(\mathrm{Tr}\left\{\sqrt{\sqrt{\rho}\sigma\sqrt{\rho}}\right\}\right)^2 . \tag{4.1}$$

This can be simplified for a pure state $\sigma = |\psi\rangle\langle\psi|$ and an arbitrary state ρ as follows:

$$F(|\psi\rangle,\rho) = \mathrm{Tr}\left\{\rho|\psi\rangle\langle\psi|\right\} \tag{4.2}$$

$$= \langle\psi|\rho|\psi\rangle . \tag{4.3}$$

The fidelity ranges from 0 to 1 and is a measure of how much two states overlap each other. If two states ρ and σ overlap each other completely ($\rho = \sigma$) the fidelity is 1. If the states do not overlap each other at all (they are orthogonal to each other) then the fidelity is 0.

We will examine how the classical schemes perform and then compare them with the quantum control scheme.

4.2 No Measurement or Correction

The first and most obvious comparison to see how well the quantum control scheme performs is to compare it to the case where we leave the state alone and hope for the best.

In this case, we take the input states

$$\rho_{\text{in1}} = |\psi_1\rangle\langle\psi_1| \tag{4.4}$$
$$\rho_{\text{in2}} = |\psi_2\rangle\langle\psi_2| \tag{4.5}$$

where

$$|\psi_1\rangle = \cos(\theta/2)|+\rangle + \sin(\theta/2)|-\rangle \tag{4.6}$$
$$|\psi_2\rangle = \cos(\theta/2)|+\rangle - \sin(\theta/2)|-\rangle \tag{4.7}$$

and apply the same noise to them as in the quantum control scheme, then see how close the noisy output states compare with the initial input states. The output states are

$$\rho_{\text{out1}} = \mathcal{E}(\rho_{\text{in1}}) \tag{4.8}$$
$$\rho_{\text{out2}} = \mathcal{E}(\rho_{\text{in2}})\,. \tag{4.9}$$

The fidelity between the input and output states is given by:

$$F_N = \langle\psi_1|\rho_{\text{out1}}|\psi_1\rangle \tag{4.10}$$
$$= \langle\psi_2|\rho_{\text{out2}}|\psi_2\rangle \tag{4.11}$$

since $\rho_{\text{in1}} = |\psi_1\rangle\langle\psi_1|$ and $\rho_{\text{in2}} = |\psi_2\rangle\langle\psi_2|$.

After some simplification, we get

$$F_N = 1 - p\cos^2\theta\,. \tag{4.12}$$

Figure 4.1 shows how F_N varies with p and θ. There are several limiting cases that are easily explained. It can be seen from figure 4.1 that when $p = 0$, the fidelity is 1 for all values of θ. This is because when there is no noise, the state does not get perturbed, and as one would expect, the output state is the same as the input state. When $\theta = \pi/2$, the fidelity is also 1 for all values of P. In this case, both states begin along the z axis and the dephasing noise rotates the state about the z

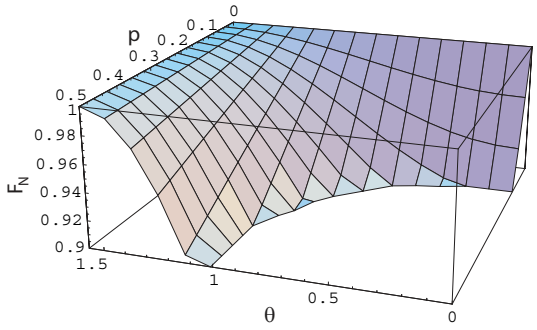

Figure 4.1: The fidelity between the input state and the noisy output state where the output state has not been measured nor corrected. Note that the z axis has been scaled to range from $0.9 - 1$. The fidelity reaches 0.5 when $p = 0.5$ and $\theta = 0$.

axis, therefore, any state along that axis will also be unperturbed. When $\theta = 0$, the noise maximally perturbs the states and when $p = 0.5$, there is a maximum amount of noise perturbing the state. This results in a completely mixed state and a fidelity of $1/2$, however we have not shown this in figure 4.1.

4.3 Discriminate-and-Replace Scheme

As discussed previously: Alice will randomly send one of two states to Bob. The state she sends will encounter some noise, therefore, a scheme which will return the noisy state as close as possible to the original pure state, is required.

The classical control strategy is to attempt to learn as much information as possible about the system. Such a scheme would consist of making a measurement to determine which state Alice sent and then recreating that state based on the results of the measurement. This requires the measurement of an observable which minimises the error about which state the system is in, that is, a measurement which distinguishes between the two states [25]. This type of measurement was first proposed by Helstrom [26] and is known a *Helstrom measurement*.[1]

4.3.1 Helstrom Measurement

In this section, we will apply the optimum discrimination measurement to our scenario [27]. Consider two states $|\psi_1\rangle$ and $|\psi_2\rangle$, in Hilbert space, each occurring with probabilities P_1 and P_2.

[1] A clear and easy to follow discussion of this is given in [27].

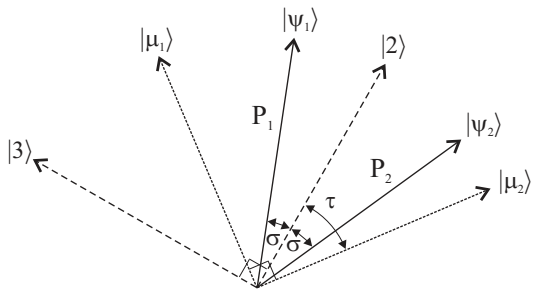

Figure 4.2: States involved in the Helstrom measurement. $|\psi_1\rangle$ and $|\psi_2\rangle$ are the input states, $|\mu_1\rangle$ and $|\mu_2\rangle$ are unknown states which make up an orthonormal basis for the optimum measurement and $|2\rangle$ and $|3\rangle$ are arbitrary basis states.

The states $|\mu_1\rangle$ and $|\mu_2\rangle$ are unknown states which make up an orthonormal basis for the optimum measurement. To be able to perform this optimum measurement, it is necessary to calculate what $|\mu_1\rangle$ and $|\mu_2\rangle$ are.

Consider two arbitrary states $|2\rangle$ and $|3\rangle$, which make up another orthonormal basis. It can be easily seen from figure 4.2 that the states $|\psi_1\rangle$, $|\psi_2\rangle$, $|\mu_1\rangle$ and $|\mu_2\rangle$ can be written in terms of this basis:

$$|\psi_1\rangle = \cos\sigma|2\rangle + \sin\sigma|3\rangle \tag{4.13}$$
$$|\psi_2\rangle = \cos\sigma|2\rangle - \sin\sigma|3\rangle \tag{4.14}$$
$$|\mu_1\rangle = \sin\tau|2\rangle + \cos\tau|3\rangle \tag{4.15}$$
$$|\mu_2\rangle = \cos\tau|2\rangle - \sin\tau|3\rangle\,. \tag{4.16}$$

The probability of making a correct measurement is given by [27]:

$$P_0 = \sum_{i=1}^{2} P_i|\langle\psi_i|\mu_i\rangle|^2 \tag{4.17}$$
$$= P_1\cos^2(\sigma-\tau) + P_2\sin^2(\sigma+\tau)\,. \tag{4.18}$$

In our scheme, the probability of Alice sending each of the states is $P_1 = P_2 = 1/2$, therefore, P_0 reduces to:

$$P_0 = \tfrac{1}{2}\Big(1 + \sin(2\sigma)\sin(2\tau)\Big) \tag{4.19}$$

To optimise the probability of making a correct measurement, we need to calculate when P_0 is maximum. Taking the derivative of P_0 with respect to τ and equating it

to zero will give a number of values for τ. The derivative is:

$$\frac{dP_0}{d\tau} = \cos(2\tau)\sin(2\sigma) \tag{4.20}$$

and is equal to zero when $\tau = \pi/4, 3\pi/4, \ldots$ This reveals the turning points of P_0, but in order to find the maxima, the negative region of the double derivative of P_0 with respect to τ is required:

$$\frac{d^2P_0}{d\tau^2} = -2\sin(2\sigma)\sin(2\tau)\,. \tag{4.21}$$

$d^2P_0/d\tau^2$ is negative when

$$\tau = \frac{\pi}{4} \quad \text{and} \quad 0 < \sigma < \frac{\pi}{2} \tag{4.22}$$

$$\tau = \frac{3\pi}{4} \quad \text{and} \quad \frac{\pi}{2} < \sigma < \pi\,. \tag{4.23}$$

The region of interest is when $0 < \sigma < \frac{\pi}{2}$, therefore we choose $\tau = \frac{\pi}{4}$ and equations 4.15 and 4.16 become:

$$|\mu_1\rangle = \frac{|2\rangle + |3\rangle}{\sqrt{2}} \tag{4.24}$$

$$|\mu_2\rangle = \frac{|2\rangle - |3\rangle}{\sqrt{2}}\,. \tag{4.25}$$

Now that we know what the measurement basis looks like in terms of our arbitrary basis, we would like to translate it into how it will look on the Bloch sphere. Rearranging equations 4.13 and 4.14, we can write the basis states $|2\rangle$ and $|3\rangle$ in terms of the states $|\psi_1\rangle$ and $|\psi_2\rangle$:

$$|2\rangle = \frac{|\psi_1\rangle + |\psi_2\rangle}{2\cos\sigma} \tag{4.26}$$

$$|3\rangle = \frac{|\psi_1\rangle - |\psi_2\rangle}{2\sin\sigma}\,. \tag{4.27}$$

We also know that the states $|\psi_1\rangle$ and $|\psi_2\rangle$ can be written as:

$$|\psi_1\rangle = \cos\tfrac{\theta}{2}|+\rangle + \sin\tfrac{\theta}{2}|-\rangle \tag{4.28}$$

$$|\psi_2\rangle = \cos\tfrac{\theta}{2}|+\rangle - \sin\tfrac{\theta}{2}|-\rangle \tag{4.29}$$

where $|\pm\rangle = (|0\rangle \pm |1\rangle)/\sqrt{2}$[2].

[2]The reader may notice that we are using the pure input states for this derivation rather than

We can now rewrite $|\mu_1\rangle$ and $|\mu_2\rangle$ in terms of states on the Bloch sphere. We make use of the fact that an angle in Hilbert space is equal to half that angle on the Bloch sphere, which in this case means that $\sigma = \theta/2$.

$$\begin{aligned} |\mu_1\rangle &= \frac{|2\rangle + |3\rangle}{\sqrt{2}} \\ &= \frac{|\psi_1\rangle + |\psi_2\rangle}{2\sqrt{2}\cos\sigma} + \frac{|\psi_1\rangle - |\psi_2\rangle}{2\sqrt{2}\sin\sigma} \\ &= \frac{\cos\frac{\theta}{2}}{\sqrt{2}\cos\sigma}|+\rangle + \frac{\sin\frac{\theta}{2}}{\sqrt{2}\sin\sigma}|-\rangle \\ &= \frac{|+\rangle + |-\rangle}{\sqrt{2}} \\ &= |0\rangle \end{aligned} \tag{4.30}$$

Similarly $|\mu_2\rangle = |1\rangle$. This corresponds to making a measurement along the z axis of the Bloch sphere. This shows that the best way to distinguish between two states symmetric about the equatorial plane is to make a measurement along the z axis of the Bloch sphere.

4.3.2 Fidelity

The probability of making a correct measurement, shown in equation 4.17, becomes:

$$P_0 = \sum_{i=1}^{2} P_i |\langle\psi_i|i\rangle|^2 \tag{4.31}$$

where $|\psi_1\rangle$ and $|\psi_2\rangle$ are defined in equations 4.28 and 4.29. This simplifies to:

$$P_0 = \tfrac{1}{2}(1 + \sin\theta)\,. \tag{4.32}$$

Using this probability, we can calculate the average fidelity for the best classical scheme.

$$F_{\mathrm{C}} = P_0 + (1 - P_0)|\langle\psi_1|\psi_2\rangle|^2 \tag{4.33}$$

$$= 1 + \tfrac{1}{2}(\sin^3\theta - \sin^2\theta) \tag{4.34}$$

where the first term in equation 4.33 refers to the probability of making a correct measurement multiplied by the fidelity when the measurement is correct (F=1);

the noisy mixed states. The justification for this will become apparent at the end of the derivation, where we find that, for this scheme, the Helstrom measurement is along the z axis and, therefore, independent of the noise p, since the noise does not affect the z component of the states. We present the derivation for pure input states as it is easier to follow, yet produces the same result.

and the second term refers to the probability of making an incorrect measurement multiplied by the fidelity when the measurement is incorrect.

Figure 4.3 shows how the fidelity depends on the angle θ. We see that the fidelity is independent of the amount of noise p. To understand why this is the case, we must consider the noise model we are using. The dephasing noise has an effect on the x and y component of the states but leaves the z component unchanged. By making the Helstrom measurement along the z axis of the Bloch sphere, the statistics of the Helstrom measurement are independent of the amount of noise. At $\theta = \pi/2$, the two states are orthogonal which means that they can be distinguished with certainty. This results in the state being recreated perfectly each time and a fidelity of 1 for all values of p. When $\theta = 0$, the states can not be distinguished, but we will always recreate the state with certainty regardless of the result of the measurement because the states begin equivalent to each other. This also results in a fidelity of 1 for all values of p.

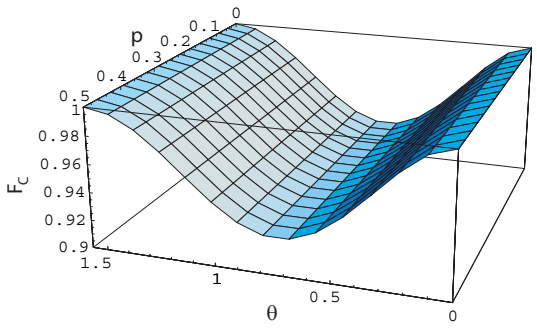

Figure 4.3: The fidelity for the discriminate-and-replace scheme.

We have calculated the fidelity between the input and output states for the case where the input state evolves under the effect of the noise with no measurement or correction; and the case where we discriminate between the two possible states and replace the state based on the results of that discrimination. We now want to calculate the fidelity for the quantum controls scheme where we avoid learning anything about the states themselves, but attempt to gain as much information as possible about the effect of the noise on the states.

4.4 Quantum Control Scheme

To characterise the quantum control scheme, we calculate the fidelity between the input state and the measured and corrected output state. Using equation 4.3, it can

be shown that the fidelity for our scheme is:

$$F_{\mathrm{QC}} = \tfrac{1}{2}\left[1 + \sin^2\theta \sin\chi + \cos\theta\sqrt{1-(1-(1-2p)^2\cos^2\theta)\sin^2\chi}\right]. \qquad (4.35)$$

We can see that F_{QC} is a function of p, θ and χ. For each p and θ, there is an optimum measurement strength χ_{opt} which gives the highest fidelity. By taking the derivative of F_{QC} with respect to χ, setting the derivative equal to zero and solving for χ, we get an expression for the optimum measurement strength χ_{opt}, which is itself a function of p and θ.

$$\chi_{\mathrm{opt}} = \arcsin\left[\frac{\sin^4\theta}{(1-(1-2p)^2\cos^2\theta)^2\cos^2\theta + (1-(1-2p)^2\cos^2\theta)\sin^4\theta}\right]^{\frac{1}{2}}. \qquad (4.36)$$

Substituting χ_{opt} for χ in equation 4.35, we get the following expression for the optimum fidelity:

$$F_{\mathrm{QCopt}} = \tfrac{1}{2}\left[1 + \sqrt{\cos^2\theta + \frac{\sin^4\theta}{1-(1-2p)^2\cos^2\theta}}\right]. \qquad (4.37)$$

Figure 4.4 shows the optimum fidelity for our quantum control scheme.

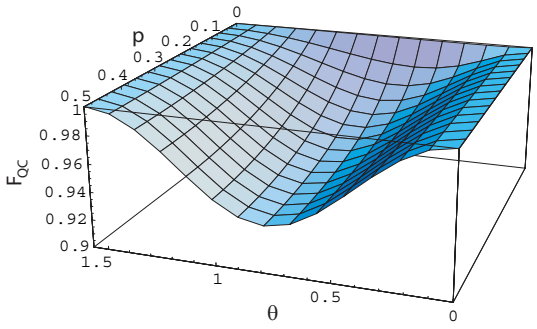

Figure 4.4: The fidelity between the input state and the measured and corrected output state for the quantum control scheme.

Notice that the fidelity is 1 for three limiting cases. When $p = 0$, there is no noise so the state is not perturbed, resulting in unity fidelity for all values of θ. When $\theta = \pi/2$, the states are orthogonal and start off along the z axis so the noise which rotates the states about the z axis does not affect the states, again resulting in unity fidelity for all values of p. To see why the fidelity is 1 for $\theta = 0$ requires a little more thought: the quantum control scheme is set up to make a measurement with the

optimum measurement strength χ_{opt}. In this case the two states are the same state and the optimum measurement is a projective measurement which will project the state into either $|+\mathrm{i}\rangle$ or $|-\mathrm{i}\rangle$. Regardless of the measurement result, the state will be pure after the measurement and when we correct the state, we rotate it about the z axis by $\eta = \pi/2$, therefore it always returns to the original state. This results in a fidelity of 1 for all values of p.

In the next section, we will compare the fidelity for the quantum control scheme to the above-mentioned schemes.

4.5 Comparing the Fidelities for the Schemes

When compared to the two schemes described in this chapter, our quantum control scheme *always* performs with an equal or higher fidelity. This can be seen in figure 4.5, where we have shown the fidelities for: a) leaving the state unmeasured and uncorrected; b) the discriminate-and-replace scheme; and c) the quantum control scheme where we do not distinguish between the states but instead use weak measurements to determine the perturbation to the state and correct it based on the measurement results.

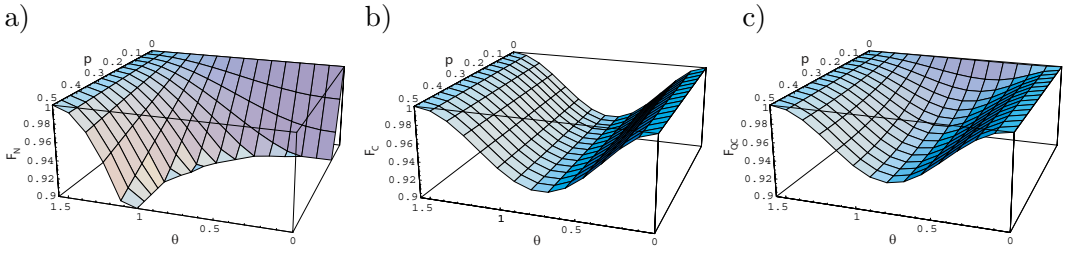

Figure 4.5: The fidelities for the three schemes that are being compared: a) sending the state through the noisy channel and doing nothing to measure and correct it; b) sending the state through the noisy channel and using the discriminate-and-replace scheme to fix it; and c) sending the state through a noisy channel and using the quantum control scheme to correct it.

To confirm that our scheme does in fact have a higher fidelity, we can take the difference between the quantum control scheme and the best of the two schemes we are comparing with.

$$F_{\text{dif}} = F_{\text{QC}} - \max(F_{\text{N}}, F_{\text{C}})\,. \tag{4.38}$$

Figure 4.6, shows that F_{dif} is always positive, which means that the quantum control scheme always has a higher fidelity. The quantum control scheme performs signifi-

cantly better in the region where $0.05 < p < 0.3$ and $0.3 < \theta < 1$, that is when there is less noise and for states which are closer together on the Bloch sphere, but not too close.

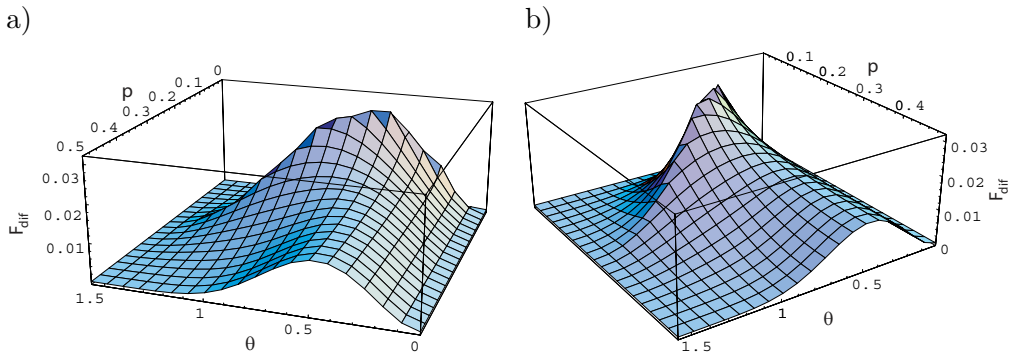

Figure 4.6: The difference between the fidelity for the quantum control scheme and the best of the two schemes being compared with the quantum control scheme: a) shows the same aspect as figure 4.5; and b) shows the same plot as a), rotated. The difference is always positive, which means that the quantum control scheme does in fact always have a higher fidelity.

In the next section we will show that our scheme not only performs better when compared to the schemes described above, but is actually the optimal quantum control scheme.

4.6 Optimal Quantum Control

We have shown that the proposed quantum control scheme performs better at protecting a quantum state than the discriminate-and-replace scheme. But is this quantum control scheme the best that we can do? The answer to that question is yes! We will show that our quantum control scheme is in fact optimal.

Throughout this thesis, we have been considering the following scenario: Alice sends one of two non orthogonal states $|\psi_1\rangle$ or $|\psi_2\rangle$ to Bob. On the way there, the state encounters some noise and becomes a mixed state ρ_1 or ρ_2. We want to find the closest physically realisable transformation to the map that takes ρ_1 and ρ_2 in the *input* Hilbert space back to $|\psi_1\rangle$ and $|\psi_2\rangle$ in the *output* Hilbert space. To do this, we need to find a linear map $\mathcal{Q}(\rho)$, which needs to be completely positive and trace-preserving (CPTP) to satisfy physical realisability, where

$$\mathcal{Q}(\rho_1) = \rho_1' \tag{4.39}$$

$$\mathcal{Q}(\rho_2) = \rho_2' \tag{4.40}$$

To optimise the map, we must maximise the average fidelity between $\mathcal{Q}(\rho)$ and the desired state [28]. This means that we want to maximise the average fidelity between the states ρ_1' and ρ_2' and the input states $|\psi_1\rangle$ and $|\psi_2\rangle$.[3] The average fidelity is:

$$\begin{aligned} F &= \tfrac{1}{2}\langle\psi_1|\rho_1'|\psi_1\rangle + \tfrac{1}{2}\langle\psi_2|\rho_2'|\psi_2\rangle & (4.41)\\ &= \tfrac{1}{2}\langle\psi_1|\mathcal{Q}(\rho_1)|\psi_1\rangle + \tfrac{1}{2}\langle\psi_2|\mathcal{Q}(\rho_2)|\psi_2\rangle\,. & (4.42)\end{aligned}$$

Using equation 2.25, we get:

$$\begin{aligned} F &= \tfrac{1}{2}\langle\psi_1|\mathrm{Tr}_{\mathrm{in}}\{(\rho_1^T\otimes I)K\}|\psi_1\rangle + \tfrac{1}{2}\langle\psi_2|\mathrm{Tr}_{\mathrm{in}}\{(\rho_2^T\otimes I)K\}|\psi_2\rangle\\ &= \tfrac{1}{2}\mathrm{Tr}_{\mathrm{out}}\{\mathrm{Tr}_{\mathrm{in}}\{(\rho_1^T\otimes I)K\}|\psi_1\rangle\langle\psi_1|\} + \tfrac{1}{2}\mathrm{Tr}_{\mathrm{out}}\{\mathrm{Tr}_{\mathrm{in}}\{(\rho_2^T\otimes I)K\}|\psi_2\rangle\langle\psi_2|\}\\ &= \tfrac{1}{2}\mathrm{Tr}\{K\rho_1^T\otimes|\psi_1\rangle\langle\psi_1|\} + \tfrac{1}{2}\mathrm{Tr}\{K\rho_2^T\otimes|\psi_2\rangle\langle\psi_2|\}\\ &= \mathrm{Tr}\{KR\} & (4.43)\end{aligned}$$

where

$$R = \tfrac{1}{2}(\rho_1^T\otimes|\psi_1\rangle\langle\psi_1| + \rho_2^T\otimes|\psi_2\rangle\langle\psi_2|)\,. \quad (4.44)$$

The problem has now been formulated as an optimisation problem where we want to

$$\begin{aligned} &\text{maximise } \mathrm{Tr}\{KR\} & (4.45)\\ &K\geq 0 & (4.46)\\ &\mathrm{Tr}_{\mathrm{out}}\{K\} = I_{\mathrm{in}}\,. & (4.47)\end{aligned}$$

This problem is non-linear and has not yet been solved analytically, however, it was shown in [28] that this type of problem belongs to a well-studied class of optimisation problems called semi-definite programs (SDP).

This problem can be cast as the *primal* problem [28], which is a minimisation of a linear function of real variable $x\in R_m$, subject to a matrix inequality:

$$\begin{aligned} &\text{minimise } c^T x\\ &F_0 + \sum_{i=1}^{m} x_i F_i \geq 0 & (4.48)\end{aligned}$$

where $F(x)$ is positive semi-definite. The problem data are $c\in R_m$ and the $m+1$ real symmetric matrices F_i. Any solution which satisfies the above constraint will give a primal value p while the minimum solution will give the optimal primal value

[3] A note on the labelling of states: When we are talking about the noise process then $|\psi_1\rangle$ and $|\psi_2\rangle$ are the input states and ρ_1 and ρ_2 are the output states. However, when we are taking about the map which takes the states ρ_1 and ρ_2 to the states ρ_1' and ρ_2' then we call ρ_1 and ρ_2 the input states and ρ_1' and ρ_2' the output states.

p^*.

Knowing the form of a primal problem, we can always reformulate it as a dual problem:

$$\begin{aligned} &\text{maximise } \mathrm{Tr}\{F_0 Z\} \\ &Z \geq 0 \qquad (4.49) \\ &\mathrm{Tr}\{F_i Z\} = c_i,\ i = 1 \ldots m \qquad (4.50) \end{aligned}$$

where the variable is the real symmetric (or Hermitian) matrix Z, and the data c. F_i are the same as in the primal problem. Any solution will give a dual value d, while the maximum will give the optimal dual value d^*.

An important property of SDPs is that they exploit the inequality

$$d \leq d^* \leq p^* \leq p\,. \qquad (4.51)$$

We will see that it is not necessary to find p^* directly. We take an educated guess at p and show that it is equivalent to d^*, then from the inequality above, the guessed p will have to be equal to p^*.

For our problem (optimising equations 4.45–4.47), the optimum dual value is given by [28]:

$$d^* \quad = \quad -2\mathrm{max}_A(\lambda_{\min}(A \otimes I - R)) + \tfrac{1}{2} \qquad (4.52)$$

where A is a traceless, Hermitian matrix and $\lambda_{\min}$ is the minimum eigenvalue of the matrix. A can be expanded in terms of the Pauli matrices:

$$A \quad = \quad aX + bY + cZ\,. \qquad (4.53)$$

We have shown numerically that $b = c = 0$, so finding d^* becomes an optimisation of a single variable a over all traceless matrices A. The quantum control scheme will give a value for p, which is related to the fidelity F_{QC}. We found that $d^* = p$ (to 10 decimal places for a 40×100 grid ranging over $0 < \theta < \pi/2$ and $0 < p < 1/2$). From the inequality in equation 4.51, if $p = d^*$ then $p = p*$, meaning that our 'guessed' p is optimal.

This result shows that our quantum control scheme is indeed optimal, meaning that there is no physical process which performs better, at returning a noisy state as close as possible to the original input state, than the proposed quantum control scheme.

4.7 Trace Distance

Using the fidelity between the input and output states, we were able to determine how well the quantum control scheme returns the noisy state as close as possible to the original input state. Now that we know that the quantum control scheme is optimal, it is of interest to investigate some other properties of the scheme.

In this section we look at a different way of characterising the schemes. We want to find how well the schemes maintain the distinguishability between the two possible states. This can be determined from the *trace distance*. The trace distance between two quantum states ρ and σ is given by:

$$D(\rho, \sigma) \equiv \frac{1}{2}\mathrm{Tr}|\rho - \sigma| \tag{4.54}$$

where $|A| \equiv \sqrt{A^\dagger A}$.

The trace distance ranges from 0 to 1 and is equal to one half of the Euclidean distance between the two states on the Bloch sphere [1]. When $D(\rho, \sigma) = 1$, the states ρ and σ are orthogonal, while when $D(\rho, \sigma) = 0$, $\rho = \sigma$. This is more intuitive if we consider the Bloch sphere. Two orthogonal states on the sphere will be on opposite surfaces of the sphere. Since the radius of the sphere is 1, the Euclidean distance between the two states will be 2, therefore the trace distance is one half of that, or 1.

We will use the trace distance to determine how well the scheme maintained the distinguishability between the two non-orthogonal input states $|\psi_1\rangle_s$ and $|\psi_2\rangle_s$. We will take the trace distance between the output states ρ_1 and ρ_2. The distinguishability between two states is higher when the trace distance between these states is higher, therefore the trace distance is related to the success probability for the Helstrom measurement.

4.7.1 No Measurement or Correction

If we let the states evolve under the dephasing noise and do nothing to correct them, then the two output states will be:

$$\rho_{N1} = \begin{bmatrix} \frac{1}{2}(1+\sin\theta) & \frac{1}{2}(\cos\theta - 2p\cos\theta) \\ \frac{1}{1}(\cos\theta - 2p\cos\theta) & \frac{1}{2}(1-\sin\theta) \end{bmatrix} \tag{4.55}$$

$$\rho_{N2} = \begin{bmatrix} \frac{1}{2}(1-\sin\theta) & \frac{1}{2}(\cos\theta - 2p\cos\theta) \\ \frac{1}{2}(\cos\theta - 2p\cos\theta) & \frac{1}{2}(1+\sin\theta) \end{bmatrix} \tag{4.56}$$

From equation 4.54, the trace distance when doing nothing to the state is:

$$D(\rho_{N1}, \rho_{N2}) = |\sin\theta| \tag{4.57}$$

and is independent of the noise p. We expect this to be the case as we know that the dephasing noise does not alter the z components of the states and therefore leaves the Euclidean distance between the states unchanged.

4.7.2 Discriminate-and-Replace Scheme

In this classical-like scheme, we make a measurement which distinguishes between the two possible input states, and replace the state based on the results of the measurement. The two output states for this scheme are:

$$\rho_{C1} = \begin{bmatrix} 1 - \frac{1}{2}\cos^2\theta & \frac{1}{2}\cos\theta \\ \frac{1}{2}\cos\theta & \frac{1}{2}\cos^2\theta \end{bmatrix} \tag{4.58}$$

$$\rho_{C2} = \begin{bmatrix} \frac{1}{2}\cos^2\theta & \frac{1}{2}\cos\theta \\ \frac{1}{2}\cos\theta & 1 - \frac{1}{2}\cos^2\theta \end{bmatrix} \tag{4.59}$$

This gives the following trace distance for the discriminate-and-replace scheme:

$$D(\rho_{C1}, \rho_{C2}) = \sin^2\theta\,. \tag{4.60}$$

The trace distance for this scheme is also independent of p as the Helstrom measurement is independent of the dephasing noise and the dephasing noise does not affect the trace distance.

4.7.3 Quantum Control Scheme

If we use the quantum control scheme to measure and correct the state, then the two output states will be:

$$\rho_{QC1} = \begin{bmatrix} \frac{1}{2}(1+\sin\theta\sin\chi) & \frac{1}{2}\cos\chi\sin\eta \\ & +(\frac{1}{2}-p)\cos\eta\cos\theta\sin\chi \\ \frac{1}{2}\cos\chi\sin\eta & \\ +(\frac{1}{2}-p)\cos\eta\cos\theta\sin\chi & \frac{1}{2}(1-\sin\theta\sin\chi) \end{bmatrix} \tag{4.61}$$

$$\rho_{QC2} = \begin{bmatrix} \frac{1}{2}(1-\sin\theta\sin\chi) & \frac{1}{2}\cos\chi\sin\eta \\ & +(\frac{1}{2}-p)\cos\eta\cos\theta\sin\chi \\ \frac{1}{2}\cos\chi\sin\eta & \\ +(\frac{1}{2}-p)\cos\eta\cos\theta\sin\chi & \frac{1}{2}(1+\sin\theta\sin\chi) \end{bmatrix} \tag{4.62}$$

$$\tag{4.63}$$

This gives the following expression for the trace distance using the quantum control scheme:

$$D(\rho_{QC1}, \rho_{QC2}) = |\sin\theta\sin\chi| \tag{4.64}$$

Any operation on two states can not make them more distinguishable [1], therefore, the optimum measurement strength to maintain the distinguishability will be one which does not measure the states at all. However, we are interested in how the trace distance will be affected when we use the optimum measurement strength which maximises the fidelity. The trace distance with $\chi = \chi_{\text{opt}}$ from equation 4.36 is:

$$D_{\text{QCopt}} = \left| \frac{\sin^3\theta}{[(1-(1-2p)^2\cos^2\theta)^2\cos^2\theta + (1-(1-2p)^2\cos^2\theta)\sin^4\theta]^{1/2}} \right| . \tag{4.65}$$

In the next section, we compare the trace distances for the three scheme mentioned above.

4.7.4 Comparing the Trace Distances for the Schemes

Using the expressions for the trace distance for the three schemes, we can see which scheme is better at maintaining the distinguishability between the two possible input states, as the initial distinguishability is the same for all schemes. Figure 4.7 shows how the trace distance, and therefore the distinguishability, compares as a function of the input state which depends on θ and the amount of noise p.

To compare the schemes quantitatively, we can find the difference between the trace distance for our scheme and the best of the trace distances for the other two schemes:

$$D_{\text{dif1}} = D_{\text{QC}} - \max(D_{\text{N}}, D_{\text{C}}) \tag{4.66}$$

$$= D_{\text{QC}} - D_N \tag{4.67}$$

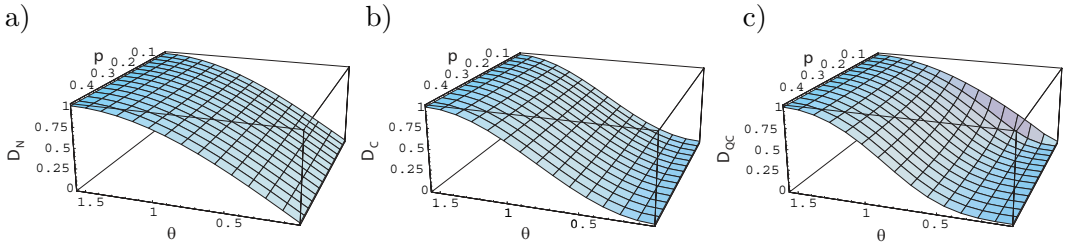

Figure 4.7: The trace distances for the three schemes that are being compared: a) sending the state through the noisy channel and doing nothing to measure and correct it; b) sending the state through the noisy channel and using the discriminate-and-replace scheme to correct it; and c) sending the state through a noisy channel and using the quantum control scheme to correct it.

where the second line turns out to be true in this case as $D_{\mathrm{N}} > D_{\mathrm{C}}$. Figure 4.8 a) shows that D_{dif1} is always negative. This means that doing nothing to measure and correct the state maintains the distinguishability between the states better than the quantum control scheme, as well as the discriminate-and-replace scheme. This is what one would expect as the noise process does not affect the z component of the states, leaving the distance between the states unchanged. As soon as we measure the states, we will cause them to become less distinguishable and since there is no process which can make two states more distinguishable, it is not possible for a scheme that measures the states to completely maintain the distinguishability between them [1].

We can, however, compare the schemes that actively control the states: the quantum control scheme and the discriminate-and-replace scheme. Taking the difference between the two schemes,

$$D_{\mathrm{dif2}} \quad = \quad D_{\mathrm{QC}} - D_{\mathrm{C}} \tag{4.68}$$

we find that the quantum control scheme is better at maintaining the distinguishability, than the discriminate-and-replace scheme, over approximately half of the parameters, as shown in figure 4.8 b) and c). While we have not explicitly compared the trace distance before noise and after the correction schemes, we know that the trace distance for the input states was the same for all schemes and therefore the scheme with the highest trace distance between the output states is better at maintaining the distinguishability. The region where our scheme performs significantly better is for a lower amount of noise ($0 < p < 0.2$) and when the states are $0.5 < \theta < 1$ apart. This region approximately corresponds to the region where the quantum control scheme also performs with a significantly higher fidelity.

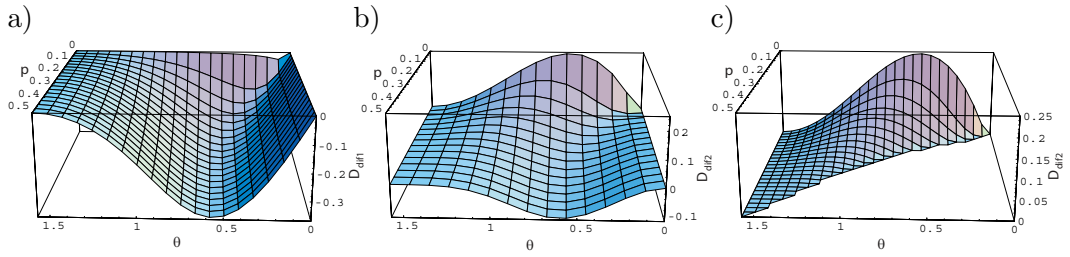

Figure 4.8: a) The difference between the trace distance for the quantum control scheme and the best of the two schemes we are comparing with the quantum control scheme. This is always negative therefore doing nothing to measure and correct the state is better for maintaining the distinguishability than the quantum control scheme. b) and c) The difference between the trace distance for quantum control scheme and the trace distance for the discriminate-and-replace scheme. We can see that for approximately half of the region of parameters, D_{dif2} is positive. a) shows all values of D_{dif2} while b) shows only the region where D_{dif2} is positive. This is the region where our scheme always performs better at maintaining the distinguishability between the two states than the discriminate-and-replace scheme.

4.8 Summary

We used the fidelity between the pure input states and the measured and corrected output states as a way of characterising the quantum controls scheme. The fidelity is a measure of how similar two states are to each other. Comparing the fidelity of the quantum control scheme to those of doing nothing to correct the state, or using a discriminate-and-replace scheme, we found that the quantum control scheme always performed with a higher fidelity. Furthermore, we showed that the quantum control scheme was in fact optimal by formulating the problem, of returning the noisy state as close as possible to the original input state, as a semi-definite program. We used the trace distance between the two possible output states as a measure of how well the schemes maintained the distinguishability between the states. Doing nothing to measure or correct the states always maintains the distinguishability between the states. The quantum control and discriminate-and-replace schemes decrease the distinguishability between the states, however the quantum control scheme performs significantly better that the discriminate-and-replace scheme over a certain range of parameters.

Chapter 5

Optical Implementation

In this chapter, we will outline how our proposed quantum control scheme can be implemented as a quantum optics experiment. We will first discuss how the schematic diagram of the quantum circuit, shown in Chapter 3, can be directly translated into an experimental setup constructed from the optical elements introduced in Chapter 2. Then we will look at what sources of optical states are available and how the dephasing noise and the feedback can be implemented in the experiment.

5.1 From Quantum Information to an Optical Circuit

To implement our quantum control scheme experimentally, we need to encode our qubits in a physical system. There are a number of ways that this can be done in optics. However, we have chosen to encode the qubits in the polarisation of single photons: a simple, easy to manipulate, two-level system. The two non-orthogonal states that Alice will prepare can be written in terms of diagonally D and anti-diagonally A polarised photons:

$$|\psi_1\rangle_s = \cos\tfrac{\theta}{2}|D\rangle + \sin\tfrac{\theta}{2}|A\rangle \quad (5.1)$$

$$|\psi_2\rangle_s = \cos\tfrac{\theta}{2}|D\rangle - \sin\tfrac{\theta}{2}|A\rangle \quad (5.2)$$

where $|D\rangle = (|H\rangle + |V\rangle)/\sqrt{2}$, $|A\rangle = (|H\rangle - |V\rangle)/\sqrt{2}$ and θ is an angle on the Poincaré sphere (see section 2.3). The subscript s denotes that this is the signal state (as opposed to the meter).

The meter state will be a horizontally polarised photon:

$$|\psi\rangle_m = |H\rangle_m \quad (5.3)$$

where the subscript m denotes that this is the meter state.

In Chapter 2, we introduced a way to construct the Pauli matrices X, Y and Z and arbitrary rotations X_θ, Y_θ and Z_θ, on polarisation encoded qubits, out of half-

wave and quarter-wave plates (HWP and QWP). We will use these wave plates to manipulate our polarised photon states the same way we manipulated the arbitrary qubit states in the previous chapters. Figure 5.1 shows the experimental setup of our quantum control scheme. The required weak measurements for this scheme have already been demonstrated by Pryde *et al.* [4].

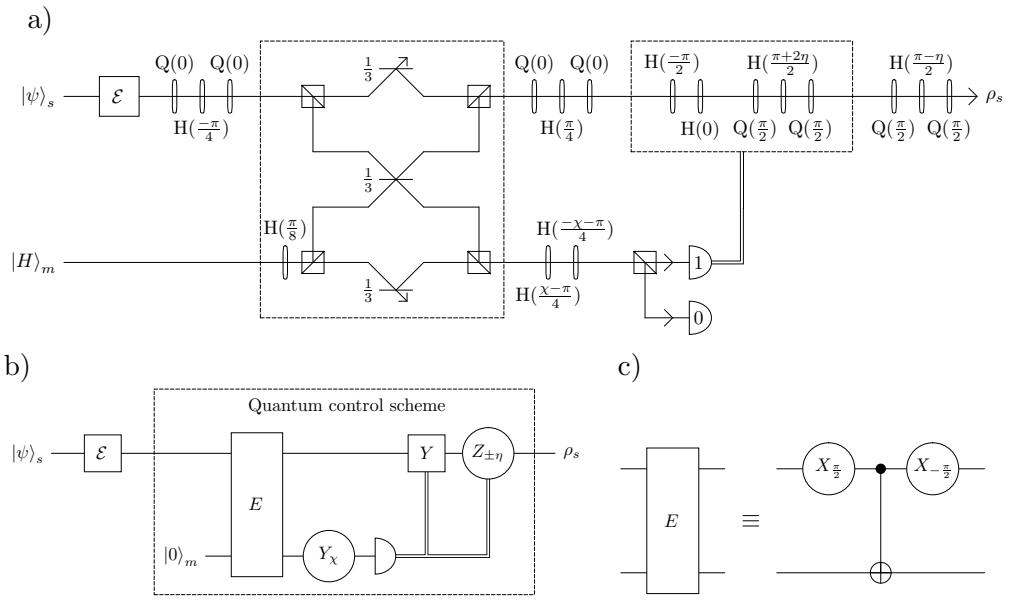

Figure 5.1: a) Schematic diagram of the proposed experimental setup for the quantum control scheme. From left to right: the first three wave plates implement an $X_{\pi/2}$ rotation on the signal photon; the elements inside the first dashed rectangle implement a CNOT gate which entangles the signal and meter photons; the three wave plates in the top rail on the right of the CNOT implement an $X_{-\pi/2}$ rotation on the signal photon and the two wave plates in the bottom rail on the right of the CNOT implement a Y_χ rotation, which determines the measurement strength, on the meter photon. The meter photon then passes through a polarising beam splitter (PBS), being detected by either detector 0 or detector 1, depending on the polarisation of the photon. The remaining seven wave plates implement the required rotations to correct the state based on the results of the detection. Figures b) and c) are the circuit diagram of the quantum control proposal, as described in Chapter 3.

The signal state $|\psi\rangle_s$ is sent through dephasing noise $\mathcal{E}$ and then entangled with the meter state $|H\rangle_m$. The entangling gate consists of: a $X_{\pi/2}$ rotation, on the signal state, which is implemented with three wave plates Q(0), H($\pi/4$) and Q(0); a CNOT which is shown in the first dotted box in figure 5.1; and a $X_{-\pi/2}$ rotation, on the signal state, which is again implemented with three wave plates Q(0), H($-\pi/4$) and Q(0). The CNOT gate is non-deterministic, which means that it does not always work; but when one photon exits from each of the outputs we know with high

probability that it has worked.

After the two states are entangled, the measurement strength is determined by a Y_χ rotation on the meter state. This is implemented with two half-wave plates H($\pi/2$) and H(0) before the meter photon's path is split by a polarising beam splitter (PBS). Depending on the polarisation of the photon, it will either be detected by detector 1 or detector 0.

Regardless of which detector detects a photon, a Z_η rotation on the signal state is implemented by three wave plates Q($\pi/2$), H($(\pi-\eta)/2$) and Q($\pi/2$) at the end of the experiment. However, if detector 1 detects a photon, there will be an additional Y and $Z_{-2\eta}$ rotation on the signal state, shown inside the dashed rectangle on the right of the diagram. These will be implemented by the five wave plates H($-\pi/2$), H(0), Q($\pi/2$), H($(\pi+2\eta)/2$) and Q($\pi/2$). This results in a rotation of Z_η on the signal photon when detector 0 detects a photon or a correction Y followed by a rotation of $Z_{-\eta}$ ($Z_{-2\eta}$ followed by Z_η) on the signal photon when detector 1 detects a photon.

5.2 Photon Sources

Currently, there are no devices that can produce a single photon on demand. There are, however, good approximations to single photon sources based on *parametric downconversion*, where pairs of photons are produced at random times. Upon detection of one photon, a good approximation to a single photon remains.

When a laser beam of frequency ω_1 is incident on a highly non-linear $\chi^{(2)}$ crystal[1], there is some probability that a high energy (pump) photon of frequency ω_p and momentum $\vec{k}_p$ will transform into a pair of lower energy (signal and idler) photons of frequency ω_s and ω_i, and momenta $\vec{k}_s$ and $\vec{k}_i$. Due to conservation of energy and momentum, the frequencies and momenta are related as follows:

$$\omega_p = \omega_s + \omega_i \tag{5.4}$$
$$\vec{k}_p = \vec{k}_s + \vec{k}_i\,. \tag{5.5}$$

In the degenerate case:

$$\omega_s = \omega_i \tag{5.6}$$
$$\vec{k}_{s_\parallel} = \vec{k}_{i_\parallel} \tag{5.7}$$
$$\vec{k}_{s_\perp} = \vec{k}_{i_\perp}\,. \tag{5.8}$$

[1] A commonly used $\chi^{(2)}$ crystal is β-barium-borate (BBO: β-BaB_2O_4). This type of crystal was used to create single photon sources in the CNOT experiment demonstrated by O'Brien *et al.* [29].

As shown in figure 5.2 a), a detector is placed in front of the two spatial modes where the photons could be.

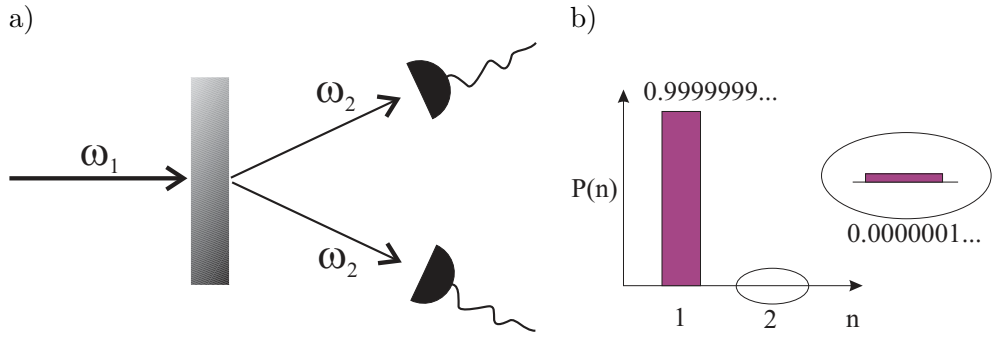

Figure 5.2: a) Conceptual diagram of parametric downconversion. A laser beam of frequency ω_1 is incident on a highly non-linear crystal.With some probability, a high energy photon from the beam will transform into a pair of lower energy photons of frequency ω_2 where, due to energy and momentum conservation, $\omega_1 = 2\omega_2$. A single photon detector is placed in front of each mode. b) When one of the detectors in a) detects a photon, then there is high probability of there being one and only one photon, and very low probability of there being two or more photons, in the other mode as depicted in the diagram.

The state that comes out will be of the form:

$$|\phi\rangle = \frac{1}{N}(|00\rangle + \lambda|11\rangle + \lambda^2|22\rangle + \lambda^3|33\rangle + \dots) \tag{5.9}$$

where N is a normalisation factor which depends on λ, and $|nn\rangle$ means that there are n photons in each mode. When a detector in front of one of the modes detects a photon, then we know with high probability that there is one and only one photon in the other mode. The second detector will detect the other photon at the end of the experiment to perform a coincidence measurement. Due to detector inefficiencies, it is possible that the detector will not be able to distinguish between whether it has detected one or two photons, so there is a chance that when the detector 'claims' to have detected only one photon, there are in fact two photons in the other mode. However, as λ is a very small number (of the order of 10^{-6}), the probability of this happening is very low. Figure 5.2 b) demonstrates how the probability of there being one photon in the other arm when the detector detects a photon compares with the probability of there being two photons in the other mode.

The input states for the quantum control scheme can be produced using the down-conversion scheme described above. The signal and idler (meter) photons will be the input photons for the quantum controls scheme. The downconversion can be set up in such a way that both the lower energy photons are horizontally polarised.

Since the meter state is $|\psi\rangle_m = |H\rangle_m$, we can pass one of the photons directly into the meter mode. To create the signal state, we need to pass the H photon through one of two half-wave plates: H$((\pi - 2\theta)/8)$ to create $|\psi_1\rangle_s$ or H$((\pi + 2\theta)/8)$ to create $|\psi_2\rangle_s$. If we want to randomly create $|\psi_1\rangle_s$ and $|\psi_2\rangle_s$ with equal probability, we can send the H photon through a 50/50 beamsplitter such that a reflected photon would be sent to one wave plate and a transmitted photon would be sent to the other wave plate.

When we detect a photon at one of the meter detectors and another photon at the output of the signal state, we know that the experiment has been successful, regardless of detector inefficiencies. However, from figure 5.1, we can see that there are a number of other paths that the photons could follow. We could get two photons at the meter detectors and no photons at the signal detector or vice versa, we could also lose photons at the 1/3 beam splitters at the top and bottom of the CNOT, to name a few. Though the experiment will run for all those cases, only the results for when the experiment was a success will be selected for analysis. This method is known as *post selection*. This means that, with current technology, the quantum control experiment will be non-deterministic.

5.3 Dephasing Noise

We will use the technique described in this section to simulate dephasing noise. The dephasing noise is deliberately added to test the quantum control protocol.

The dephasing noise consists of applying a phase flip Z on the state with some probability p and doing nothing to the state with probability $1 - p$. One possible way to implement this experimentally is using a Pockels cell (PC) [31]. When a photon is sent through a PC, nothing happens to it unless a voltage is applied to the cell. When this voltage is applied, the photon experiences a phase shift, between the horizontal and vertical components, of a set value which can range from 0 to 2π. In our case, we would want a phase shift of π. The PC can be connected to a random number generator with the appropriate statistics for the experiment.

5.4 Feedback and Correction

After being entangled with the signal photon, the meter photon passes through a polarising beam splitter. Depending on the polarisation of the photon, it is detected by either detector 0 or 1. The correction in this experiment could be implemented using a number of PCs triggered by the detection of a photon at detector 1. The PCs will need to apply the transformations shown in the dotted box on the right of figure 5.1.

The feedback process will most likely be much slower than the time it takes for the signal photon to leave the entangling gate and arrive at the point where it needs to be corrected. The signal photon can be delayed by sending it through a fibre optic cable, giving the feedback process enough time to activate the PCs.

This type of feedback and correction has been recently demonstrated by Pittman *et al.* [31], where the feedback was used in an experimental demonstration of a quantum error correction.

5.5 Characterisation

To characterise the experimental scheme, one can employ quantum state tomography to completely reconstruct the density matrices of the input and output states. This is done by making a series of measurements on a large number of identically prepared copies of the quantum systems. This method was used by O'Brien *et al.* [30] to characterise the performance of the CNOT demonstrated by O'Brien *et al* [29]. Knowing the density matrices for the states, we can calculate the fidelity between the two input and output states to see how well the scheme has performed.

5.6 Summary

The quantum control scheme described in Chapter 3 can be implemented as a quantum optics experiment by encoding the qubits in the orthogonal polarisations of a single photon. All the necessary one qubit gates can be implemented using combinations of half and quarter-wave plates, and the entangling gate uses the CNOT proposed in [3, 29]. The states can be prepared with high probability using parametric downconversion while the dephasing noise and feedback control can be implemented with the use of Pockels cells. The experimental scheme can be characterised by performing state and process tomography on the experiment. In addition, all of the required operations have already been demonstrated experimentally.

Chapter 6

Conclusion

The theory and application of classical control is already well developed. In this thesis, we have taken the first steps in formulating a quantum control theory for single qubits as well as proposing an experiment to test the theory.

The main ideas behind classical control are that of measurement, feedback and correction. This poses a problem for quantum control as the measurement of a quantum system will necessarily introduce back-action noise into that system. In addition, quantum mechanics introduces the concept of non-orthogonal states and there exists no measurement which can deterministically distinguish two non-orthogonal states with certainty.

In this thesis, we have discussed the theory of a number of different types of quantum measurements. Quantum non-demolition (QND) measurements make use of an ancillary (meter) system which is entangled with the state of interest (the state of the signal system). A measurement of the state of the meter system will give information about the state of the signal without destroying the signal system. QND measurements are projective, which means that while they do not destroy the state of interest, they do project it into an eigenstate of the measurement. Weak measurements, however, allow the measurement strength to be varied by varying the state of the meter. The strength of the measurement ranges from no measurement being made when the measurement is 'turned off' to a strong measurement where the measurement is a projective QND measurement. There is a trade-off between the amount of information gained about the state of the system and the disturbance to the system. We have shown that somewhere in between, there is an optimum measurement strength which gives sufficient information about the state while minimising the disturbance to the system.

The proposed quantum control scheme uses weak measurements to determine the effect of the noise on the state, then correct the state based on the results of the measurement. The input state is one of two non orthogonal states. The states are non-orthogonal to ensure that they can not be distinguished with certainty. The correction of orthogonal, and therefore distinguishable, states would not require the

use of the quantum control scheme. In this scheme one party, Alice, randomly sends one of these two non-orthogonal states to another party, Bob. Before reaching Bob, the state will inevitably encounter some noise, which we have modelled as dephasing noise. Using a CNOT, we entangle the signal state to a meter state. The measurement strength is then determined by a Pauli-Y rotation on the meter state which is subsequently measured by a detector. Based on the results of this measurement, the signal state is corrected by a Pauli-Z rotation.

To characterise how well the scheme has performed, we use the fidelity between the input and output signal states. The fidelity is a measure that determines how similar two states are to each other and ranges from 0 (for orthogonal states) to 1 (for identical states). We compare the fidelity for our scheme with the fidelities for two other schemes: in the first scheme, we let the state evolve under noise and do nothing to measure or correct it; and in the second scheme we use the a classical-like discriminate-and-replace scheme. We have shown that the fidelity for our scheme is always higher than the fidelity for either of the schemes we used for comparison. In addition, we have shown that our scheme is the optimal quantum control scheme to return the noisy state to as close as possible to the original pure state, by formulating the problem as a semi-definite program. We have also investigated the ability of the quantum controls scheme at maintaining the distinguishability between the two possible input states.

We have shown that the proposed quantum control scheme can be implemented experimentally by encoding the qubits in the orthogonal polarisation of single photons. All the necessary rotations can be implemented by a number of half-wave and quarter-wave plates. We also presented a brief discussion into the available single photon sources for state preparation, the dephasing noise and a possible feedback scheme.

In this thesis, we have only considered one iteration of the quantum control scheme. Many, if not all, control schemes utilise repeated or continuous measurement and correction of a system. A future direction may be to consider multiple iterations of this scheme where the measured and corrected output state encounters more noise and is measured and corrected again. It may be worthwhile to also consider making the correction based not only on the measurement results of each iteration, but on the results of all past measurements, as discussed in [15].

We believe that quantum control will play a necessary role in the quest for further technological advances. In this thesis, we have made the first steps toward formulating the theory of quantum control for single qubits.

References

[1] M. A. Nielsen and I. L. Chuang, *Quantum Information and Computation*, Cambridge University Press, Cambridge (2000).

[2] P. Grangier, J. A. Levenson, and J.-P. Poizat, Nature (London) **396**, 537 (1998).

[3] T. C. Ralph, S. D. Bartlett, J. L. O'Brien, G. J. Pryde, and H. W. Wiseman, quant-ph/0412149

[4] G. J. Pryde, J. L. O'Brien, A. G. White, S. D. Bartlett, and T. C. Ralph, Phys. Rev. Lett. **92**, 190402 (2004).

[5] C. M. Caves, K. S. Thorne, R. W. P. Drever, V. D. Sandberg, and M. Zimmermann, Rev. Mod. Phys. **52**, 341 (1980).

[6] M. F. Bocko and R. Onofrio, Rev. Mod. Phys. **68**, 755 (1996).

[7] V. Belavkin, Rep. Math. Phys. **43**, 405 (1999).

[8] C. M. Caves and G. J. Milburn, Phys. Rev. A **36**, 5543 (1987).

[9] H. M. Wiseman and G. J. Milburn, Phys. Rev. Lett.**70**, 548 (1993).

[10] L. K. Thomsen, S. Mancini, and H. M. Wiseman, Phys. Rev. A **65**, 061801 (2002).

[11] J. M. Geremia, J. K. Stockton, and H. Mabuchi, Science **304**, 270 (2004).

[12] J. M. Geremia, J. K. Stockton, A. C. Doherty, and H. Mabuchi, Phys. Rev. Lett. **91**, 250801 (2003).

[13] G. Welsh and G. Bishop, *An Introduction to the Kalman Filter* (2004) Available: `http://www.cs.unc.edu/~welch/media/pdf/kalman_intro.pdf` 18/05/2005.

[14] W. P. Smith, J. E. Reiner, L. A. Orozco, S. Kuhr, and H. M. Wiseman, Phys. Rev. Lett. **89**, 133601 (2002).

[15] A. C. Doherty and K. Jacobs, Phys. Rev. A **60**, 2700 (1999).

[16] A. Jamiołkowski, Rep. Math. Phys. **3**, 275 (1972).

[17] M.-D. Choi, Linear Algebra and its Applications, **10**, 285 (1975).

[18] J. Fiurášek, Phys. Rev. A **66**, 052315 (2002).

[19] T. B. Pittman, M. J. Fitch, B. C. Jacobs, and J. D. Franson, Phys. Rev. A **68**, 032316 (2003).

[20] S. Gasparoni, J.-W. Pan, P. Walther, T. Rudolph, and A. Zeilinger, Phys. Rev. Lett. **93**, 020504 (2004).

[21] Z. Zhao, Y.-A. Chen, A.-N. Zhang, T. Yang, H. Briegel, and J.-W. Pan, Nature (London) **430**, 54 (2004).

[22] M. Koashi, T. Yamamoto, and N. Imoto, Phys. Rev. A **63** 030301 (2001).

[23] Hans-A. Bachor and Timothy C. Ralph, *A Guide to Experiments in Quantum Optics*, WILEY, Weinheim (2004).

[24] N. K. Langford,"Performing Arbitrary Unitary Operations with Wave Plates", unpublished.

[25] C.A. Fuchs and M. Sasaki, quant-ph/0302092

[26] Carl A. Helstrom, *Quantum Detection and Estimation Theory*, Academic Press, New York (1976).

[27] A. Chefles, quant-ph/0010114

[28] K. Audenaert and B. De Moor, quant-ph/0109155

[29] J. L. O'Brien, G. J. Pryde, A. G. White, T. C. Ralph, and D. Branning, Nature (London) **426**, 264 (2003).

[30] J. L. O'Brien, G. J. Pryde, A. Gilchrist, D. F. V. James, N. K. Langford, T. C. Ralph, and A. G. White, Phys. Rev. Lett. **93**, 080502 (2004).

[31] T. B. Pittman, B. C. Jacobs, and J. D. Franson, quant-ph/0502042